



# Long-term chemical characterization of tropical and marine aerosols at the Cape Verde Atmospheric Observatory (CVAO) from 2007 to 2011

K. W. Fomba, K. Müller, D. van Pinxteren, L. Poulain, M. van Pinxteren, and H. Herrmann

TROPOS – Leibniz Institute for Tropospheric Research, Permoserstr. 15, 04318 Leipzig, Germany

Correspondence to: H. Herrmann (herrmann@tropos.de)

Received: 29 November 2013 – Published in Atmos. Chem. Phys. Discuss.: 14 February 2014

Revised: 7 July 2014 – Accepted: 23 July 2014 – Published: 1 September 2014

**Abstract.** The first long-term aerosol sampling and chemical characterization results from measurements at the Cape Verde Atmospheric Observatory (CVAO) on the island of São Vicente are presented and are discussed with respect to air mass origin and seasonal trends. In total 671 samples were collected using a high-volume PM<sub>10</sub> sampler on quartz fiber filters from January 2007 to December 2011. The samples were analyzed for their aerosol chemical composition, including their ionic and organic constituents. Back trajectory analyses showed that the aerosol at CVAO was strongly influenced by emissions from Europe and Africa, with the latter often responsible for high mineral dust loading. Sea salt and mineral dust dominated the aerosol mass and made up in total about 80 % of the aerosol mass. The 5-year PM<sub>10</sub> mean was  $47.1 \pm 55.5 \mu\text{g m}^{-2}$ , while the mineral dust and sea salt means were  $27.9 \pm 48.7$  and  $11.1 \pm 5.5 \mu\text{g m}^{-2}$ , respectively. Non-sea-salt (nss) sulfate made up 62 % of the total sulfate and originated from both long-range transport from Africa or Europe and marine sources. Strong seasonal variation was observed for the aerosol components. While nitrate showed no clear seasonal variation with an annual mean of  $1.1 \pm 0.6 \mu\text{g m}^{-3}$ , the aerosol mass, OC (organic carbon) and EC (elemental carbon), showed strong winter maxima due to strong influence of African air mass inflow. Additionally during summer, elevated concentrations of OM were observed originating from marine emissions. A summer maximum was observed for non-sea-salt sulfate and was connected to periods when air mass inflow was predominantly of marine origin, indicating that marine biogenic emissions were a significant source. Ammonium showed a distinct maximum in spring and coincided with ocean surface water chlorophyll *a* concentrations. Good correlations were also observed be-

tween nss-sulfate and oxalate during the summer and winter seasons, indicating a likely photochemical in-cloud processing of the marine and anthropogenic precursors of these species. High temporal variability was observed in both chloride and bromide depletion, differing significantly within the seasons, air mass history and Saharan dust concentration. Chloride (bromide) depletion varied from  $8.8 \pm 8.5$  % ( $62 \pm 42$  %) in Saharan-dust-dominated air mass to  $30 \pm 12$  % ( $87 \pm 11$  %) in polluted Europe air masses. During summer, bromide depletion often reached 100 % in marine as well as in polluted continental samples. In addition to the influence of the aerosol acidic components, photochemistry was one of the main drivers of halogenide depletion during the summer; while during dust events, displacement reaction with nitric acid was found to be the dominant mechanism. Positive matrix factorization (PMF) analysis identified three major aerosol sources: sea salt, aged sea salt and long-range transport. The ionic budget was dominated by the first two of these factors, while the long-range transport factor could only account for about 14 % of the total observed ionic mass.

## 1 Introduction

The interest in research on atmospheric aerosols is not only limited to heavily polluted megacities and other strongly anthropogenically polluted areas; also concerns naturally mobilized dust and sea salt aerosols which are in the focus of marine chemistry, biology and atmospheric chemistry (Raes et al., 2010; Radhi et al., 2010; Heller and Croot, 2011; Carpenter et al., 2004; Quinn and Bates, 2005; Formenti et al.,

2011). The creation and operation of the Cape Verde Atmospheric Observatory (Observatório Atmosférico de Cabo Verde: Humberto Duarte Fonseca, CVAO) in 2006, located on São Vicente Island, was a joint activity of British, German and Cape Verdean scientific institutes with funding from the European Union (EU), national scientific projects and institutions. On the one hand, the CVAO is downwind of the Mauritanian coastal upwelling region off northwest Africa, an area of high marine biological productivity. Observations made at the CVAO therefore provide information on links between atmospheric compositional changes, marine biology and climate. On the other hand, satellite, ground-based, ship and aircraft measurements have shown the outflow of Saharan dust into the Atlantic Ocean usually across the Cape Verde islands (Chiapello et al., 1999; Formenti et al., 2003; Reid et al., 2003; Tesche et al., 2011; Gelado-Caballero et al., 2012), making them a suitable location for characterizing mineral dust. The station is situated at the far edge of the island in the direction of air mass inflow to the island so that air masses observed at the station are free from local pollution, thereby making the station suitable for also performing remote marine aerosol experiments. The atmospheric deposition of nutrients that are derived from dust – such as nitrogen, phosphorus and iron compounds – into the oceans plays a crucial role in marine biogeochemical cycles and in some areas establishes a major nutrient input to the open oceans (Cropp et al., 2005; Ohde and Siegel, 2010; Bates et al., 2001). The role of desert aerosols in atmospheric processes strongly depends on a variety of physicochemical parameters and their spatial distribution and transformations in the atmosphere (Kelly et al., 2007; Lee et al., 2010).

During late spring and summer, the CVAO site mostly receives North Atlantic marine air masses along the NNE trade winds, which, although sometimes influenced by the Mauritanian upwelling, provide the possibility for long-term studies of “background” Atlantic air and its associated trace gases of oceanic origin. During late fall and winter, Cape Verde is situated in the direct transport pathway of Saharan dust from Africa to the North Atlantic. During this season dust is transported in the lower troposphere and the deposition takes place mainly over the eastern tropical Atlantic (Schepanski et al., 2009) and Cape Verde.

In principle, atmospheric chemistry in this region of the Cape Verde Islands is expected to be influenced by emissions from the ocean (Mahajan et al., 2010; Read et al., 2008); Saharan dust; and anthropogenically released gases and particles from continental Africa, southwestern Europe and in minor cases North American sources.

The investigation of the role of mineral dust in the ocean has been the focus of a number of research and ship cruises along the tropical Atlantic Ocean (Bates et al., 2001; Chen and Siefert, 2003; Allan et al., 2009). However, these measurements have mostly focused on short-term measurements during intensive field campaigns that last for 3–6 weeks, making predictions about seasonal variability and long-term un-

derstanding of atmospheric processes quite difficult. Such long-term data sets have been often requested (Mahowald et al., 2005), but only a few data actually exist for the region of the tropical North Atlantic (e.g., Kandler et al., 2007; Chiapello et al., 1995). Chiapello et al. (1995) collected filter samples over 3 years for metal analyses at the Cape Verde island Sal from a region that was far from the coastline and influenced by the island itself. There are also some data from ship cruises and short-term experiments near this region (Chen and Siefert, 2004; Rijkenberg et al., 2008; Kandler et al., 2011). Long-term observations were made in the subtropical region at Izaña (Tenerife) 1500 km NNE from São Vicente, but Izaña is located at 2373 m a.s.l. (above sea level) and Santa Cruz is influenced heavily by local pollution (Alastuey et al., 2005). Long-term measurements in a remote site in the eastern tropical North Atlantic Ocean are not known. In a recent study (Schulz et al., 2012), a marine atmospheric monitoring network for long-term observations of dust transport and deposition to the ocean was asked for as well as encouraged for future harmonized activities in marine aerosol research. The measurements at the CVAO intend to improve on the present data scarcity and also meet other expectations.

Within the present study the long-term PM<sub>10</sub> high-volume filter measurements at the CVAO are discussed. The presented results aim to deliver the first long-term data set of aerosol chemical composition for further use, e.g., in marine biogeochemistry research and for marine aerosol modeling, where long-term experimental data on the aerosol constitution and its size-resolved chemical composition are needed. The results are focused on samples collected since the creation of the CVAO in 2007 until the end of 2011. The aspects addressed are particulate mass concentrations, chloride depletion, concentration of ionic components, organic matter (OM) and elemental carbon (EC). The mineral dust fraction of the aerosol particles and its seasonal and interannual variability are also discussed. Back trajectories were used to classify typical source regions. Related works from the CVAO include first investigations from short-term experiments of PM characterization (Fomba et al., 2013; Müller et al., 2010) and of specific organic single compounds (Müller et al., 2009).

## 2 Experimental

### 2.1 Site and sampling

Sampling was done at the CVAO, which is located at the northeastern shore of the island of São Vicente in Cape Verde. The sampling site is situated 70 m from the coastline (16°51'49 N, 24°52'02 W) about 10 m a.s.l. This region experiences constant northeastern winds from Africa through the Canary Islands. The average annual temperature at the CVAO is 23.6 ± 4.0 °C, and it is an arid region with a maximum of 24–350 mm rainfall per year. The precipitation frequency is about 3 to 10 events per year mainly between August and

October. Therefore, the wet deposition of particles in this region is negligible. A more detailed description of the meteorological conditions can be found (Carpenter et al., 2010). Sample collection was performed on top of a tower with an inlet height of 32 m to reduce the direct influence of sea spray on the collected particles. Due to the location of the station, influences from the island like orographic influences in dust sedimentation and anthropogenic emissions are negligible. Thus the collected samples are representative of a clean atmosphere over the ocean and not contaminated by gases or particulates from the island itself. However, though such events are very rare, during southwesterly winds influences from the island could be observed.

All background meteorological data, temperature, relative humidity and wind measurements were collected from 31 and 10 m heights at a frequency of 1 Hz, then averaged over 1 min and 10 min to hourly values. Atmospheric pressure and broadband UV radiation were recorded at a 4 m height.

Particle sampling was done using a high-volume (HV) collector with a PM<sub>10</sub>-inlet (Digital filter sampler DHA-80, Walter Riemer Messtechnik, Germany) that was operated with an average flow rate of 500 l min<sup>-1</sup> in a 24 h sampling period during intensive campaigns and was switched to 72 h sampling period otherwise. The high-volume samples were collected on acquired 150 mm preheated quartz fiber filters (Munktell, MK 360) and were further preheated in our laboratory at 110 °C for 24 h to get rid of the OC background content. Our unpublished results of tests at higher temperatures delivered similar blanks, but the mechanical stability of the filters (abrasion and breaking resistance) was better when handling at 110 °C.

After sampling, the filters were stored at 5 °C and subsequently cooled and transported to a freezer. The long-term storage and transportation of the collected filters from the CVAO to Germany was always carried out in aluminum boxes at -20 °C.

## 2.2 Laboratory analysis

The filters were equilibrated for 72 h under constant temperature (20 ± 1 °C) and humidity (50 ± 5 %) before and after collection and weighed using a microbalance (Mod. AT261 Delta Range, Mettler-Toledo, Switzerland) with a reading precision of 10 µg.

For ion analysis, 25 % of the PM<sub>10</sub> quartz fiber filter was extracted with 30 ml Milli-Q water (> 18 MΩ cm, 15 min shaker, 15 min ultrasonic bath, 15 min shaker). Sample extracts were filtered through a 0.45 µm one-way syringe filter to remove insoluble materials prior to ion analysis. The ion analysis was performed for cations Na<sup>+</sup>, NH<sub>4</sub><sup>+</sup>, K<sup>+</sup>, Mg<sup>2+</sup>, Ca<sup>2+</sup> and anions Cl<sup>-</sup> and Br<sup>-</sup>, NO<sub>3</sub><sup>-</sup>, SO<sub>4</sub><sup>2-</sup> and C<sub>2</sub>O<sub>4</sub><sup>2-</sup> using a standard ion-chromatography technique (ICS3000, DIONEX, USA) equipped with an automatic eluent generation (KOH for anions and methanesulfonic acid (MSA) for cations) and a micromembrane suppression unit. For the an-

**Table 1.** HV filters collected at the CVAO from 2007 to 2011.

	2007	2008	2009	2010	2011
Total amount	105	105	154	148	159
72 h samples	45	69	66	105	85
24 h samples during intensive campaigns	60	36	88	43	74
Collected at 32 m	105	105	132	50	159
Collected at 4 m			22	98	

ion separation a combination of AG18 and AS18 (2 mm) was applied, while for the cation separation CG16 and CS16 (3 mm) were used. Chromatographic calibrations were carried out daily using a four-point standard (Fluka, Switzerland). The detection limits for all ions measured by conductivity detection were within 0.002 µg m<sup>-2</sup> except for calcium, which was 0.02 µg m<sup>-2</sup>. Bromide was detected using UV/VIS detection (VWD-1, Dionex) with a detection limit of 0.001 µg m<sup>-3</sup>. Analyzed field blank filters were used for blank correction via subtraction. Non-sea-salt sulfate (nss-sulfate) was determined from the subtraction of sea salt sulfate (ss-sulfate) from the total sulfate. Ss-sulfate was determined from the stable ratio SO<sub>4</sub><sup>2-</sup> / Na<sup>+</sup> = 0.251 (Liebezeit, 2011) in sea water under the assumption that sodium has no other sources.

Organic and elemental carbon were analyzed by a two-step thermographic method (C-mat 5500, Ströhlein, Germany) with nondispersive infrared sensor (NDIR) detection as described in the following literature: Neusüss et al. (2002), Gnauk et al. (2008) and Carpenter et al. (2010). The detection limits for quartz fiber filter analysis were 30 ng m<sup>-3</sup> for EC and 100 ng m<sup>-3</sup> for OC. For the determination of OM (organic matter) the estimation of Turpin (Turpin et al., 2000) was applied with OM considered as twice OC (OM = 2 × OC), which is recommended for aged aerosols. In previous studies, results of single organic compounds were presented (Müller et al., 2009, 2010; Alastuey et al., 2005), while in the present work only oxalic acid concentrations shall be discussed.

Air mass back trajectory analyses were performed to assist in the data interpretation and to provide useful hints on various air mass origins. Back trajectories ensembles (van Pinxteren et al., 2010) were calculated (starting 500 m above ground) using the NOAA HYSPLIT (HYbrid Single-Particle Lagrangian Integrated Trajectory, <http://www.arl.noaa.gov/ready/hysplit4.html>) model.

## 2.3 Positive matrix factorization (PMF) analysis

Source apportionment of the analyzed aerosol chemical composition (OC, EC, Na<sup>+</sup>, NH<sub>4</sub><sup>+</sup>, K<sup>+</sup>, Mg<sup>2+</sup>, Ca<sup>2+</sup>, Cl<sup>-</sup>, Br<sup>-</sup>, NO<sub>3</sub><sup>-</sup>, SO<sub>4</sub><sup>2-</sup> and C<sub>2</sub>O<sub>4</sub><sup>2-</sup>) was performed using the multilinear engine algorithm (ME-2) developed by Paatero (1999). Results were analyzed according to the ME-2 graphic

interphase Sofi from Canonaco et al. (2013). Since positive matrix factorization (PMF) is a weighted least squares method, individual estimates of uncertainties associated with each data value are required. In this work the uncertainties were obtained from the calibration uncertainties of the main ions and OC/EC that were applied on the measured concentrations. The PMF was run using two to five factors, and each factor solution was evaluated using the seed. It was found that the three-factor solution could explain the data most appropriately and thus provided the most meaningful results (Fig. S2 in the Supplement). The obtained solution was interpreted on the basis of the air mass back trajectories, the meteorological conditions and the chemical composition of the filters. Further details on the results of the different factors can be found in the Supplement.

### 3 Results

#### 3.1 Back trajectory analysis

Hourly back trajectory analyses were performed for more than 600 samples. In general, 96 h back trajectory ensembles were calculated. The plots represent a trajectory ensemble consisting of 648 single back trajectories calculated for a 24 h time interval of the individual samples. For a few sampling periods, longer back trajectories were calculated for a better understanding of possible sources since submicron particles could have longer atmospheric lifetimes (Jaenicke, 1980) depending on the height (Williams et al., 2002). The most important air mass origins were classified as follows (Fig. 1):

- (A) The air mass spent the last 96 h over the Atlantic Ocean and was from the North Atlantic or western North Atlantic Ocean (16.5 % of all samples).
- (B) The air mass spent less than 48 h over the ocean in the last 96 h before arriving at CVAO and originated from the African continent, crossing over the Saharan, urban sites (Nouakchott, Dakar, etc.) as well as biomass burning regions through the Mauritanian upwelling region to the CVAO (22.2 % of all samples).
- (C) Air masses from the Atlantic Ocean crossing the Mauritanian upwelling region, partially NW Africa, Canary Islands (26.3 % of all samples).
- (D) Air masses which originated from or in SW Europe and crossed the Mauritanian upwelling region, coastal areas in NW Africa and/or the Canary Islands and the eastern North Atlantic Ocean (17.7 % of all samples).
- (E) All further back trajectories (17.3 % of all samples) that could not be assigned to the above four major classes. This includes air masses that reached the CVAO from western Africa (south of the Sahara), the equatorial Atlantic Ocean and from North America.

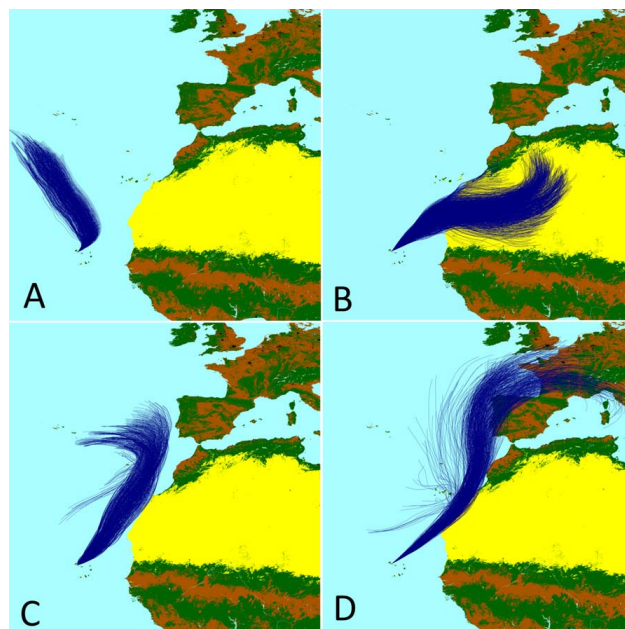


**Figure 1.** Typical 96 h air mass back trajectory ensembles calculated for CVAO during the routine filter sampling periods; aerosol type and  $\text{PM}_{10}$  mass concentration are given in parentheses: (a) 2 May 2011: marine air mass from the North Atlantic Ocean (mass,  $m = 8.28 \mu\text{g m}^{-3}$ ); (b) 14 January 2011: Saharan air mass (dust loaded,  $m = 155.04 \mu\text{g m}^{-3}$ ); (c) 12 July 2008: slightly polluted air mass from the northwestern African coast and the Canary Islands,  $m = 21.61 \mu\text{g m}^{-3}$ ; and (d) 2 February 2011: air mass from Europe crossing the coastline of NW Africa and the Canary Islands (anthropogenically influenced,  $m = 64.89 \mu\text{g m}^{-3}$ );

Late fall and winter are the typical dust seasons at the Cape Verde islands. During this time easterly and northeasterly winds transport Saharan dust into the tropical eastern Atlantic. During spring and summer, the air mass origin is mainly marine, but sometimes the trade winds cross the African coast in Morocco and Western Sahara and at times originate from the Iberian Peninsula. Equatorial air masses rarely reach the Cape Verde archipelago.

#### 3.2 Chemical characterization of the aerosol constituents

A total of 671 samples were collected and analyzed for their chemical composition over the stated time period. Table 1 shows the overview of the total number of investigated samples in this work during the investigated time period. The observed difference in the number of collected filters between the years is related to the different sampling routines that were implemented. During the first 4 months of sampling in 2007, the samples were collected as 72 h samples within 1 week in the regime of 3 h sampling and 4 h sampling break. After the first intensive campaign (May/June 2007) during which sample collection was done for 24 h without a break

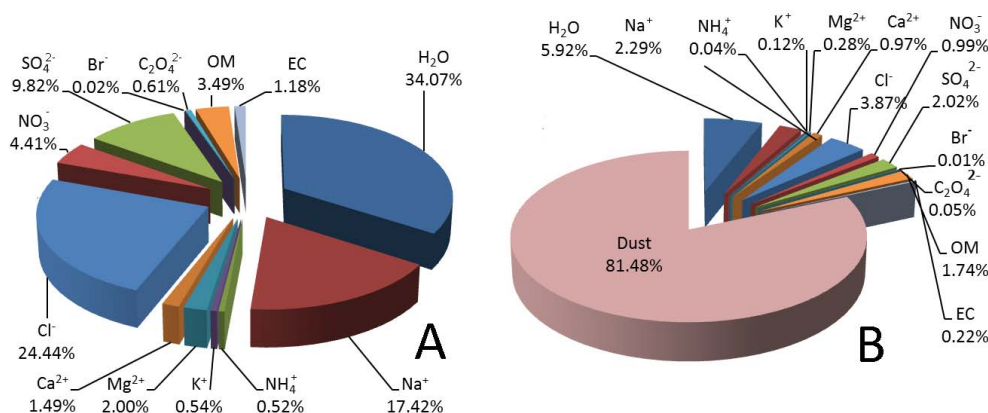


**Figure 2.** Averaged PM<sub>10</sub> constitution for 183 marine samples (a) and 49 mineral-dust-dominated aerosol samples (b) collected at 32 m on top of the tower.

between filter sampling, the collection was changed to 3 days continuous sampling and 3 days pause within the time period of August 2007 and December 2008. Afterwards the sampling period was fixed at 72 h without a break. A few exceptions to this sampling regime were caused by power failures at the CVAO and sampler defect in July/August 2009 (cf. Table 1). This explains the higher number of filters observed in 2009 to 2011 in comparison to 2007 and 2008. From October 2009 to July 2010 samples were collected on top of a container due to the reconstruction of the tower. At the lower sampling height (4 m) the direct sea spray from the nearby coastline influenced the aerosol constitution enormously. In these samples the sea salt concentration was about four to five times higher than in samples collected from the top of the tower.

### 3.2.1 Mineral dust estimation and marine aerosol

The estimation of the mineral dust content in the aerosol samples was achieved by the subtraction of all determined species, including the estimated mass of water, from the total mass. This was done as a first approximation since major mineral dust component such as Al, Si or Fe were not measured due to technical reasons. Thus, the mineral dust assumed here is analogous to the rest of the undetermined aerosol component and is thus considered as the maximum possible dust concentrations. The water content of the samples was estimated via the E-AIM (Extended Aerosol Inorganics Model) III of Clegg et al. (1998). This model, however, delivers higher water content values than the application of a hydration multiplication factor of 1.29 to the mass of all water-soluble inorganic compounds as suggested later (Harrison et al., 2003; Sciare et al., 2005). Using Clegg's model, the average aerosol water concentration was  $5.7 \pm 3.4 \mu\text{g m}^{-3}$ . The uncertainty obtained due to the application of this model was less than 10% ( $0.5 \mu\text{g m}^{-3}$ ) in the estimated water content. The estimated error had a negli-

ble effect on the estimated dust concentrations since the value was far smaller compared to the uncertainty related to the determination of the other measured ions. Mineral dust, which in this region was mostly Saharan dust, was the most dominant component of the particulate matter, with a 5-year average of  $25.8 \pm 51.1 \mu\text{g m}^{-2}$ , equivalent to about 55% of the total average aerosol mass concentration. Strong temporal and seasonal variations were observed for the dust concentrations, with concentration ranging from 0 to  $575.6 \mu\text{g m}^{-3}$ .

The highest dust concentration was found during the winter season due to frequent Saharan dust events that were strongly influenced by the Harmattan, a characteristic wind transporting Saharan dust in lower heights to the Atlantic Ocean between the end of November and the beginning of March. A few heavy-dust events were observed in spring and fall but not in the summer. In general, differences were found in the aerosol chemical composition during days of and days without dust storms.

The mean aerosol composition of Saharan-dust-dominated samples corresponding to aerosol mass concentrations higher than  $90 \mu\text{g m}^{-3}$  and that of marine-aerosol-dominated days with aerosol mass less than  $20 \mu\text{g m}^{-3}$  are shown in Fig. 2. Both situations had same chemical components – including water-soluble ions, organic and elemental carbon, water and mineral dust – with different fractional composition. As would be expected aerosol water was lower during dust storms than during marine-influenced days. Sea salt concentrations did not change significantly during and without dust storms. However, the relative contribution of sea salt was higher in marine-influenced air masses than in Saharan dust air masses.

Higher concentrations were also observed for sulfate, nitrate, EC/OM, and the crustal elements such as potassium and calcium during dust events as compared to marine-influenced days. However, their relative compositions during dust events were lower than during marine-influenced days due to the total absolute mass. During the non-dust period,

**Table 2.** Minimum, maximum, 5 year average and standard deviations ( $\mu\text{g m}^{-3}$ ) of  $\text{PM}_{10}$  aerosol components at CVAO.

Components	Min	Max	Mean	Median	SD
Mass load	4.00	601.83	47.20	30.10	55.50
Dust	0.00	575.56	25.90	9.70	51.10
Sea salt	0.71	39.67	11.00	10.71	5.10
$\text{Cl}^-$	0.35	21.17	5.70	5.43	2.70
$\text{Br}^-$	Bdl	0.25	0.005	0.003	0.01
$\text{NO}_3^-$	0.14	3.76	1.10	1.00	0.60
$\text{SO}_4^{2-}$	0.31	7.38	2.50	2.33	1.20
$\text{C}_2\text{O}_4^{2-}$	Bdl	0.46	0.08	0.06	0.10
$\text{Na}^+$	0.25	12.74	3.70	3.72	1.70
$\text{NH}_4^+$	Bdl	0.76	0.09	0.05	0.10
$\text{K}^+$	Bdl	0.86	0.13	0.13	0.10
$\text{Mg}^{2+}$	0.05	1.34	0.40	0.37	0.20
$\text{Ca}^{2+}$	Bdl	4.44	0.64	0.46	0.60
OM (OC*2)	Bdl	6.67	1.02	0.67	1.04
EC	Bdl	1.32	0.13	0.08	0.16

Bdl: below detection limit; SD: standard deviation

long-range transport from the northwestern African coast and Europe, and secondarily formed PM from the ocean were the main sources of nss-aerosol constituents.

### 3.3 Temporal and seasonal variations

Results of the measured chemical components are shown in Table 2, including their 5-year averages, minima and maxima. This is the first unique data set of nearly continuously collected PM from the Cape Verde archipelago and in the region of the tropical North Atlantic over a time period of 5 years. In the following, the temporal and seasonal variations of the PM constituents are discussed with respect to the meteorological conditions and air mass origin. Figure 3 shows the time series of some of the investigated chemical components within the stated time period. The red lines represent the time period during which sample collection was performed on top of a container, while the blue lines represent measurements that were performed on the 30 m tall tower.

#### 3.3.1 $\text{PM}_{10}$ mass concentration

During the 5 years of PM collection at the 32 m sampling height an average mass concentration of  $47.1 \pm 55.5 \mu\text{g m}^{-3}$  was observed. Aerosol mass showed strong variability with minimum and maximum values of  $4.0 \mu\text{g m}^{-3}$  and  $601.8 \mu\text{g m}^{-2}$ , respectively (Table 2). The highest and lowest daily mean concentrations were observed in January 2008 and March 2009, respectively. Low concentrations were observed during days with low wind speeds of remote Atlantic Ocean air mass inflow, and/or after precipitation events, which typically occurred in the fall. The highest aerosol mass was observed during days of Saharan dust storm when air

mass crossed the Saharan prior to their arrival at CVAO. Table 3 shows an overview of the mass concentration of the number of samples sampled during different seasons. At the CVAO, particle mass concentration was a good indicator of the aerosol mineral dust content. Typically, mass concentrations below  $20 \mu\text{g m}^{-2}$  were observed during marine air mass inflow (Fig. 1a). When aerosol mass concentrations were between 20 and  $90 \mu\text{g m}^{-2}$ , the air mass originated from any of the three above-mentioned air mass classes (C to E), as shown in Fig. 1b–d, or also of marine origin with higher wind speeds. The only exception was observed when the samples were collected at a 4 m height, during which sea salt concentrations increased dramatically and the above-mentioned features did not hold. The spikes in the  $\text{PM}_{10}$  profile as shown in Fig. 3, corresponding to mass concentrations above  $90 \mu\text{g m}^{-3}$ , were indicative of days where aerosol mass was dominated by Saharan dust (Fig. 1b). On average, such strong Saharan dust events were observed about 11–19 times a year. The duration of Saharan dust events varied from 1 to 10 days, with the longest event also supported by back trajectory analysis observed from the 25 December 2007 to 4 January 2008.

The interannual variation of the monthly mean of the  $\text{PM}_{10}$  mass concentration and seasonal variation of some chemical aerosol components are shown in Fig. 4. The highest mass loadings were observed in 2008 and the lowest in 2009. A strong seasonal trend was found in the mass loadings. The average mass concentrations were  $71.8 \pm 34.3$ ,  $33.7 \pm 15.3$ ,  $36.5 \pm 10.3$  and  $43.7 \pm 12.6 \mu\text{g m}^{-3}$  for winter, spring, summer and fall, respectively. The highest temporal variation was observed during the winter season due to frequent change in air mass inflow. The lowest mass concentrations were observed in the spring season (April to June) despite some episodic dust events during this period (e.g., May 2007), while the highest concentrations were observed during the late fall and winter (December to February).

Similar seasonal trends were reported by Chiapello et al. (1995) for the island of Sal despite their more continental location on the island whereby anthropogenic activities could strongly affect mass loadings. According to Schepanski et al. (2009) the Sahara produces larger amount of dust during summer, but the dust is transported at higher altitudes of up to 10 km within the Sahara Air Layer, while in winter the dust is transported along the northeast trade winds at far lower altitudes. Thus the higher amounts of Saharan dust together with anthropogenic gaseous and particulate compounds from the African continent are responsible for the winter elevated  $\text{PM}_{10}$  mass concentrations, while marine and non-African air mass inflow were responsible for low mass loadings.

#### 3.3.2 Sea salt

Sea salt concentration was estimated as  $1.17 \cdot ([\text{Na}^+] + [\text{Cl}^-])$  (Anguelova, 2002). The temporal variation of sea salt concentrations is shown in Fig. 3.

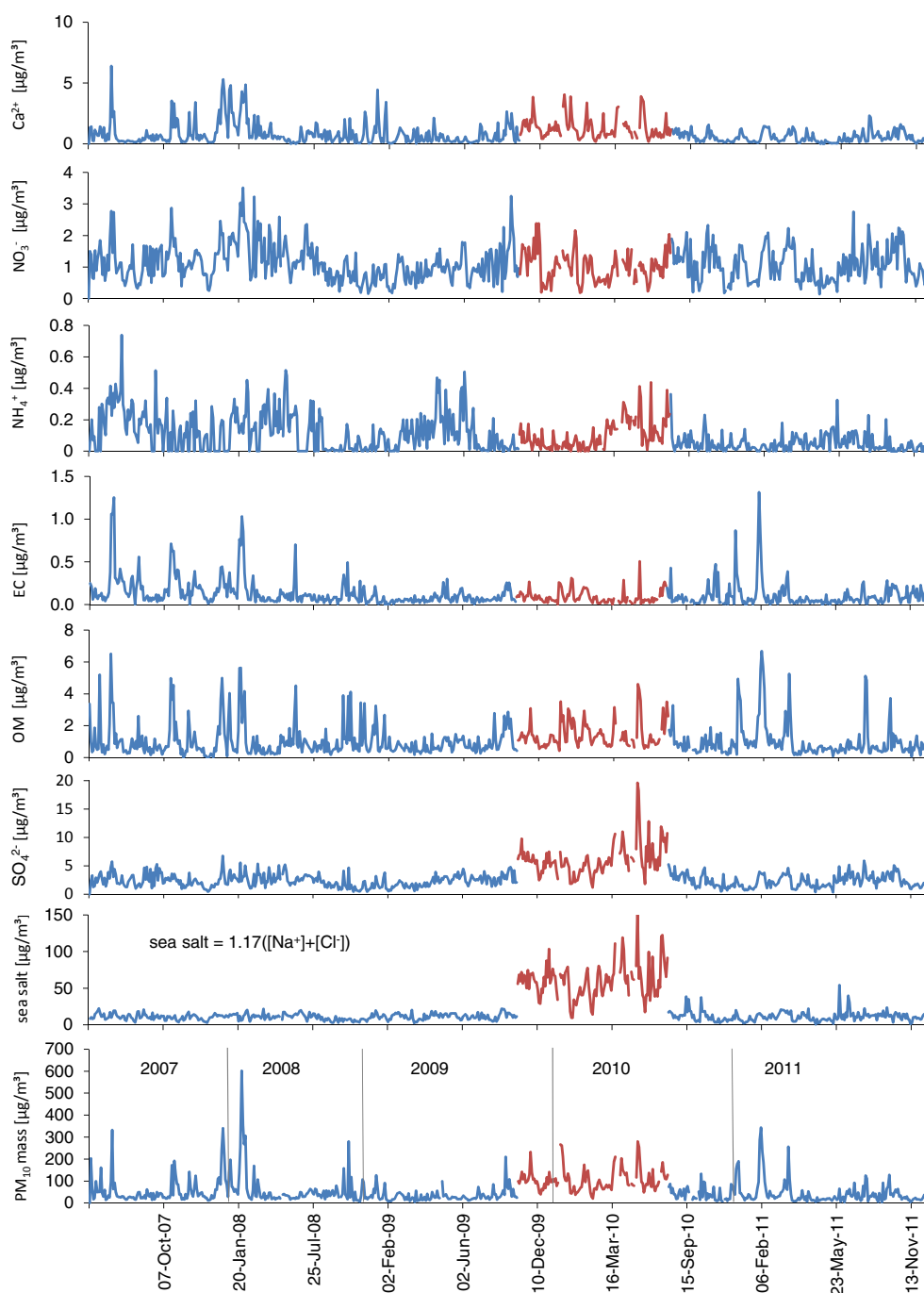


**Figure 3.** Time series of mass concentration and major  $PM_{10}$  aerosol components in filter samples collected during the 5 years from 2007 to 2011. During the period from 23 October 2009 till 09 July 2010 (red line) all samples were collected on top of a storage container with an inlet height of 4 m above ground; all other samples were collected on top of the tower with an inlet height of 32 m above ground.

The observed concentration of sea salt was strongly dependent on the meteorological conditions and the sampling height. The averaged wind speed at the CVAO was about  $7.3 \text{ m s}^{-1}$ , while the maximum wind speed observed was about  $13 \text{ m s}^{-1}$ . During days with high wind speeds the sea salt concentrations increased strongly. The highest wind

speeds were often combined with air masses coming from North America crossing the northern Atlantic to CVAO. This observation was made after the back trajectory analysis and it is valid for the majority of these events.

During such days, the aerosol mass was slightly higher than in days with lower ( $< 4 \text{ m s}^{-1}$ ) wind speed or dominant

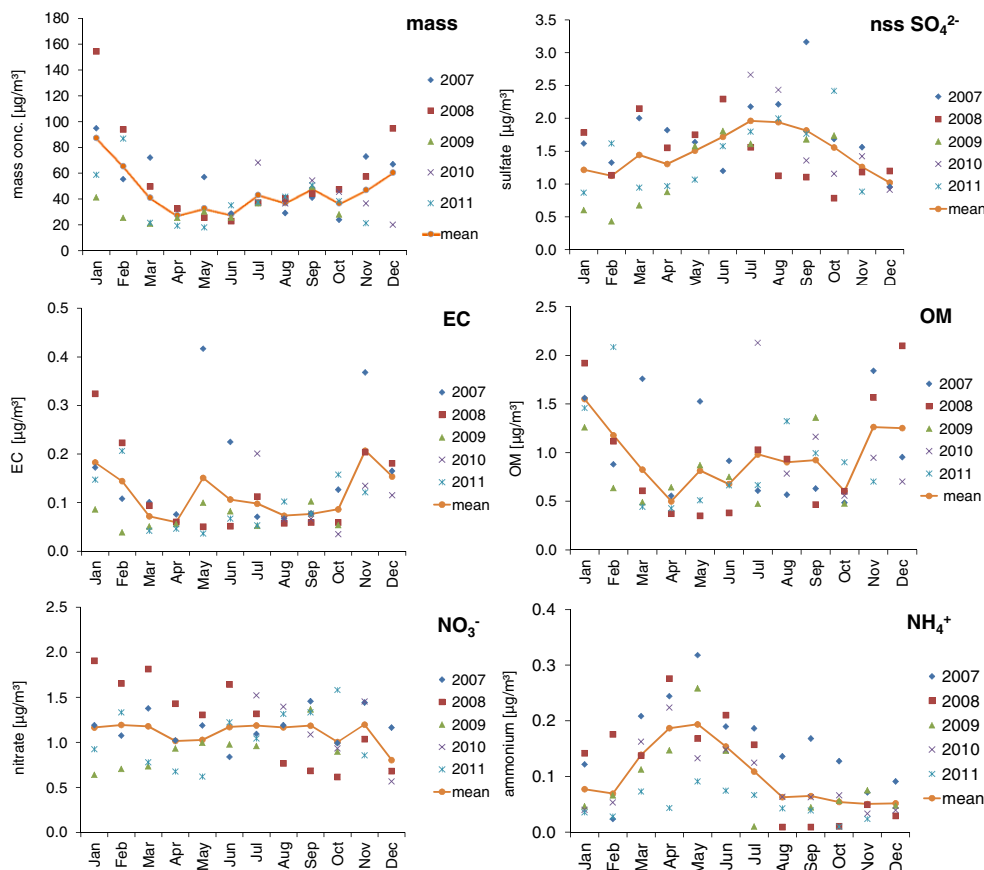


**Figure 4.** Annual variability and monthly mean of  $\text{PM}_{10}$  mass concentration, non-sea-salt sulfate, elemental carbon (EC), organic matter (OM), nitrate and ammonium during the 5 years of measurements for samples collected on the tower.

**Table 3.** Seasonality of  $\text{PM}_{10}$  particle mass concentration collected with a DHA-80 HV filter sampler between January 2007 and November 2011 on top of the tower\*.

Season	Mar–May	Jun–Aug	Sep–Nov	Dec–Feb	Total
Mass: $> 200 \mu\text{g m}^{-3}$	2	0	1	15	18
Mass: $90\text{--}200 \mu\text{g m}^{-3}$	7	4	10	22	43
Mass: $20\text{--}90 \mu\text{g m}^{-3}$	62	98	91	98	349
Mass: $< 20 \mu\text{g m}^{-3}$	47	22	19	41	129
Total samples	118	124	121	176	539

\* Samples collected between 23 October 2009 and 9 July 2010 were not included here because of the lower sampling height on the container roof.

marine air mass inflow. The averaged sea salt concentration was  $11.1 \pm 5.5 \mu\text{g m}^{-2}$  in samples collected on top of the tower and  $58.3 \pm 28.3 \mu\text{g m}^{-3}$  for samples collected at the 4 m sampling height. Sea salt and other sea-spray-associated aerosol components increased enormously (about a factor of 4–5) at the lower sampling height. This was due to the fact that sample collection at 4 m height was done within the internal marine boundary layer (Niedermeier et al., 2014) whereby aerosol mass was mostly affected by the surf zone. Increases in sea salt concentrations were observed during

days of high wind speeds, but a strong correlation between sea salt and the local wind speed was not observed. According to de Leeuw et al. (2000) and Niedermeier et al. (2014), sea salt concentrations may increase significantly at wind speeds above  $10 \text{ ms}^{-1}$  depending on the wind direction and the oceanic waves. The highest sea salt concentration determined at the tower was  $54 \mu\text{g m}^{-3}$  in spring 2011 in an episode when the local wind speed was  $13 \text{ ms}^{-1}$ . The temporal variability of sea salt was not as strong as compared to those of mineral dust and aerosol mass. No seasonal trend

was observed in the sea salt concentrations, and the Mg / Na ratio found in the dust (0.12) and non-dust (0.11) samples was similar to the ratio in sea salt (0.12), implying no influence of the dust storms on sea salt and particularly on sodium concentrations.

### 3.3.3 Sulfate

Sulfate consisted of ss-sulfate and of nss-sulfate mainly of secondary origin. In Fig. 3, the temporal variability of the total sulfate concentration is presented. Sea salt sulfate had a similar temporal trend to sea salt; thus, the variations observed in the time series are attributed to variations in nss-sulfate concentration. On the average, ss-sulfate made up only 38 % of the total sulfate measured at the tower. This, however, increased when sampling was done at a lower height. The highest sulfate concentrations were strongly connected to Saharan dust events, but not all dust events were responsible for the elevated sulfate concentrations. When air mass containing dust did not have contact with anthropogenic SO<sub>2</sub> pollution sources, the nss-sulfate was not elevated and vice versa. During the dust season, marine sources of nss-sulfate played a minor role. The averaged nss-sulfate concentration in winter marine air masses was  $0.47 \pm 0.31 \mu\text{g m}^{-3}$ , while for the dust days the averaged nss-sulfate concentration was  $2.46 \pm 1.05 \mu\text{g m}^{-3}$ . The strong increase in sulfate concentrations during the dust events is indicative of anthropogenic activities in Africa that influences the aerosol composition. Natural sources of SO<sub>2</sub> are unlikely since the only nearby natural source is the ocean and nss-sulfate secondarily produced from oceanic precursors would therefore not vary significantly with air mass origin. In Fig. 4 the interannual and seasonal variation of nss-sulfate is given. The average monthly concentration ranged from  $0.43$  to  $3.0 \mu\text{g m}^{-3}$ , with higher concentrations observed during the summer months especially during July and August. A unique source for this high summer concentration has not been identified. However, the increased photochemical activity during the summer as compared to the winter months and the changes in the emission of dimethyl sulphide (DMS) due to higher biological activities in the ocean could possibly influence the measured nss-sulfate concentration.

Elsewhere, seasonal trends have been observed for methanesulfonic acid (MSA) and DMS, which are known precursors of nss-sulfate with higher concentrations observed in the summer than in the winter (Sciare et al., 2009). It has also been reported (Kouvarakis and Mihalopoulos, 2002; Kettle et al., 1999) that sea surface water temperature influences the production of nss-sulfate and other organic materials in the ocean surface microlayer (SML), leading to pronounced seasonal cycle in nss-sulfate concentrations, with the maximum observed in summer and the minimum in winter. Studies in the Mediterranean Sea (a region with relatively high anthropogenic pollution) have evaluated the biogenic contribution to nss-sulfate concentration to be between 6 and

22 % (Ganor et al., 2000; Mihalopoulos et al., 1997). It has also been observed that under marine air mass conditions the contribution of biogenic sources to nss-sulfate may rise up to 100 % (Bates et al., 1992). At the CVAO, the minimum concentration of nss-sulfate during the winter and the summer was about  $0.20$  and  $0.70 \mu\text{g m}^{-2}$ , respectively. As a first approximation, assuming that these lowest concentrations of nss-sulfate were of biogenic contribution from the ocean, this would imply that the biogenic contribution to the total nss-sulfate could be estimated to be, on average, about  $40 \pm 20$  % in this region. Thus, although anthropogenic activities influence nss-sulfate concentrations especially during dust storms and air mass coming from Europe via the Moroccan coast, photochemical production of nss-sulfate and emission of marine precursors could also have been important during the summer in this region.

### 3.3.4 OM and EC

These two carbon sum parameters showed a good correlation in their time series. The 5-year average for OM and EC was  $1.02 \pm 1.04$  and  $0.13 \pm 0.16 \mu\text{g m}^{-3}$ , respectively. The observed EC value was quite similar to the annual mean of  $0.18 \mu\text{g m}^{-3}$  found by T. Nunes (personal communication, 2013) for the year 2011 on the island of Santiago, which is a slightly more anthropogenically influenced region than the CVAO. Figure 3 shows the variability in both EC and OM concentration over the investigated time period. Elevated EC concentrations were strongly connected to elevated OM concentration but not vice versa. The number of samples with elevated OM concentration was greater than those with elevated EC concentration because of additional natural single sources of OM, especially during the summer. High concentrations of OM and EC were strongly correlated to air masses originating from the African continent.

During the Harmattan season (end of November to middle of March) aerosols from the African continent carried not only Saharan dust but also anthropogenic emissions from ship tracks near the African coast, the African coastal cities of Dakar and Nouakchott, and sometimes biomass burning aerosols (EC and OM) as well as biological material into the Cape Verde region (Milton et al., 2008). During such periods the EC concentration was three times higher than in air masses coming from Europe and 5 times higher than in marine air masses. The lower transport height is a further important factor for the measured elevated concentrations of dust and other aerosol components during the winter season. The averaged concentration of EC and OM given in Table 2 were in the same range as those recently reported for marine environments (Alves et al., 2007). The lowest concentration for EC was found in dominant marine air masses.

It has been reported that biogenic-material-containing organic substances of low solubility in the upper sea water layer are emitted via the SML into the atmosphere and are found mainly in submicron particles (O'Dowd and De

Leeuw, 2007; Facchini et al., 2008; Müller et al., 2009). Secondary organic aerosols formation from marine sources has also been reported in a different marine environment (Kawamura and Gagosian, 1987; O'Dowd et al., 2004; Facchini et al., 2010). In Fig. 4, the monthly and interannual variation of OM and EC are presented. A strong seasonal trend is observed for OM and EC, with higher values observed during the winter seasons than otherwise. This winter maximum is similar to that observed for the mass concentration, and it is attributed to the influence of continental air masses from Africa, which often carries a lot of Saharan dust as well as anthropogenically emitted particles. Beside the anthropogenic sources of OM and EC, OM was also emitted from the SML of the ocean itself. The amount of the marine OM production depends on oceanic biological activity, which has a distinct seasonality (Sciare et al., 2009). A smaller summer maximum of OM (Fig. 4) was also observed which had its origin from direct marine emissions or in marine emissions of gaseous precursors of PM, such as DMS, isoprene, organic amines and others (Gantt et al., 2011; Gantt and Meskhidze, 2013). The lowest OM concentrations were observed in April and October at CVAO. With the exception of the high values observed for EC in May 2007, which was due to a dust storm during this month, the EC values remain low throughout the other seasons. Thus, the high EC concentration in this region was mostly due to long-range transport from Africa in the dust season.

### 3.3.5 Nitrogen-containing ions

Ammonium and nitrate showed no correlation with one another. These ions might have had other sources. The 5-year average of ammonium and nitrate was  $0.09 \pm 0.1$  and  $1.1 \pm 0.1 \mu\text{g m}^{-3}$ , respectively. Clarke and Porter (1993) and Quinn et al. (1988) found similar ammonium concentration in remote oceanic regions and suggested it could be of marine biogenic origin. The concentration of both ions (ammonium and nitrate) was not influenced by the sampling height, implying their content in sea salt is very low. Nitrate-like ammonium also showed strong temporal variation (Fig. 3). Ammonium concentrations varied from below the detection limit to  $0.76 \mu\text{g m}^{-3}$ , while nitrate concentrations varied from  $0.14$  to  $3.7 \mu\text{g m}^{-3}$  (Table 2). This strong variation was attributed to the changing air mass origin. In marine air masses the nitrate concentration was lower than in air masses coming from the African or European continent, implying long-range transport was a significant source of the observed nitrate concentrations. For ammonium, summer concentrations were found to be 44 % higher than the winter concentrations for clean marine air masses, which would suggest that marine biological and photochemical processes could strongly influence the ammonium concentrations in this region.

Nitrate concentrations, however, never showed a strong seasonal trend as shown in Fig. 4. A slight increase in the nitrate concentrations (about 20 %) was often observed in

the summer except during 2008m where a strong decline in nitrate concentrations from January to December was observed. Ammonium, on the other hand, showed seasonal trends with annual maximum observed in spring and early summer (Fig. 4). As can be observed in Fig. 4, ammonium seasonality was not correlated with either the aerosol mass loading or the nss-sulfate trend. This suggests that the observed ammonium in this region is not strongly linked to ammonium sulfate and may have another major source different from long-range transport from the continent. Marine sources of  $\text{NH}_3$  were reported earlier by Jickells et al. (2003) from isotopic measurements. Quinn et al. (1988) also observed simultaneously high concentrations of ammonia in the Pacific Ocean and in the ocean's atmosphere and indicated that the ocean was the potential source of the ammonia. They observed an averaged ammonium concentration of about  $108 \text{ ng m}^{-3}$  in the remote eastern North Pacific Ocean in May, which is on the same order of magnitude as that observed at CVAO during May:  $165 \pm 129 \text{ ng m}^{-3}$ . Clarke and Porter (1993) have also shown good correlation between atmospheric ammonium and chlorophyll *a* concentrations. Although long-range transport cannot be neglected, our results indicate that the ocean has a significant contribution to the observed ammonium especially during the spring in this region.

### 3.3.6 Calcium

Calcium showed strong temporal variation throughout the year depending on the air mass origin and sampling height (Fig. 3). This variation indicates that calcium was from both sea spray and mineral dust, corresponding to sea salt (ss) and nss-calcium. The calcium peaks were correlated with either peaks in aerosol mass loading or sea salt concentrations. The minimum and maximum concentrations were  $0.01$  and  $4.44 \mu\text{g m}^{-3}$ , respectively. The maximum and minimum values were related to days of Saharan dust events and days of dominant marine air mass inflow, respectively. A strong correlation between nss-calcium and total soluble calcium (with  $r^2 = 0.98$ ) during dust events confirmed that the Saharan dust was the main source of nss-calcium in these samples. Thus, soluble nss-calcium was often a good indicator of Saharan dust in this region. Calcium-rich aerosol was often mobilized from the NW Sahara. During the atmospheric transport the insoluble  $\text{CaCO}_3$  was processed to more soluble compounds, e.g., in clouds. Sea salt and mineral dust contributed  $0.15 \pm 0.15$  and  $0.49 \pm 0.48 \mu\text{g m}^{-3}$ , respectively, to the total soluble calcium average concentration of  $0.64 \pm 0.63 \mu\text{g m}^{-3}$ .

### 3.3.7 Potassium and magnesium

Variations in potassium and magnesium concentrations were also attributed to the varying air mass inflow and the different sampling height with maximum concentrations of potassium and magnesium observed at 0.86 and

**Table 4.** Comparison of published averaged oxalate concentration in PM<sub>10</sub> aerosols with the results of this study.

Sampling site	Sampling interval	Oxalate [ $\mu\text{g m}^{-3}$ ]	Reference
CVAO, marine non-polluted	Winters 2007–2011	$0.07 \pm 0.06$	This study
CVAO, marine non-polluted	Summers 2007–2011	$0.06 \pm 0.05$	This study
CVAO, continentally influenced	2007–2011	$0.12 \pm 0.06$ (Africa) $0.12 \pm 0.05$ (Europe)	This study
Amsterdam Island	2003–2007	$0.0003\text{--}0.017$	Rinaldi et al. (2011)
Mace Head	2006	$0.0027\text{--}0.039$	
Tropical to western North Pacific	Sep–Dec 1990	0.040	Kawamura and Sakaguchi (1999)
Tropical Atlantic	April 1996	$0.052 \pm 0.030$	Johansen et al. (2000)
Atlantic Ocean 25° N–4° S	November 1999	$0.074 \pm 0.048$	Virkkula et al. (2006)
Hong Kong	December 2000	0.35	Yao et al. (2002)
Sapporo, Japan	August 2005	0.196	Pavuluri et al. (2012)

$1.34 \mu\text{g m}^{-3}$ , respectively (Table 2). The 5-year average concentrations at the tower of potassium and magnesium were  $0.13 \pm 0.09$  and  $0.40 \pm 0.20 \mu\text{g m}^{-3}$ , respectively, of which nss-potassium and nss-magnesium made up only  $0.02 \pm 0.06$  and  $0.02 \pm 0.04 \mu\text{g m}^{-3}$  of the total average, respectively. This corresponds to only about 10 % of potassium and 5 % of magnesium. Thus the ocean was the main source of these ions in this region. Nss-potassium peaks were often linked with nss-calcium and mass loading peaks, implying continental air masses from Africa could account for some of the nss-potassium concentrations found in this region.

### 3.3.8 Oxalate

Oxalate concentrations were low in comparison to those reported in urban and continental aerosols. Table 4 shows an overview of the measured oxalate concentration and those of other reported works. The average oxalate concentration during polluted air masses was about  $0.12 \pm 0.06 \mu\text{g m}^{-3}$ . This value was twice as much as the concentrations observed during marine air mass inflow. Comparatively to reported oxalate concentrations (Table 4), the observed concentrations were within reported range. The values were higher than those reported in other marine environments such as in Mace Head or Amsterdam Island (Rinaldi et al., 2011) but lower than those reported in continental aerosols such as in Hong Kong (Yao et al., 2002) or Sapporo, Japan (Pavuluri et al., 2012). The differences between the results in this study and the abovementioned works is strongly related to the different air mass inflow regions in these areas. Mace Head is more remote than CVAO, while Hong Kong and Sapporo are more urban than CVAO.

In general, elevated oxalate concentrations were observed in polluted European and African air masses (Table 4). The maximum oxalate concentration was measured at  $0.46 \mu\text{g m}^{-2}$  in September 2009 during a period where air mass originated from western Africa. During the Saharan-dust-influenced winter days, the oxalate concentration was

higher than during non-dust winter days. The high values were usually connected to dust storms, while peaks in oxalate concentrations during the summer season were connected to periods of high photochemical activity; periods of high marine activities, whereby potential oxalate precursors could have been emitted to the atmosphere; and periods when other precursors that might have been transported from Europe. A distinct seasonality in oxalate concentration was observed with a maximum during the summer season (June to August). The formation of oxalate depends on the presence of organic precursors, such as ethene (Warneck, 2003), glyoxal (Carlton et al., 2007) and sunlight, which are more available during the summer.

In general, the aerosol chemical composition was influenced by sea salt; organic compounds emitted from the ocean surface microlayer; organic matter; and long-range-transported particulate matter or precursors from anthropogenic emissions in northwestern Africa, the Canary Islands and the European continent. The Cape Verde islands themselves were only a minor source of PM because of the prevailing northeast trade winds and the location of the CVAO at the northeastern shore of the island São Vicente.

## 3.4 Inter-relationship between ionic species

### 3.4.1 Nitrate and nss-sulfate

Nitrate and nss-sulfate showed good correlations during the winter and the summer ( $r^2 = 0.72$ ) seasons (November–April and May–October, Fig. 5), which could be attributed to their anthropogenic origin due to observation of frequent elevation of these concentrations during long-range transport from Europe and Africa.

The higher slope of the regression line during summer in comparison to that of winter is indicative of the presence of an additional source of nss-sulfate such as the production through photochemical processes. In principle, both ions in the particle phase or their gas phase precursors might

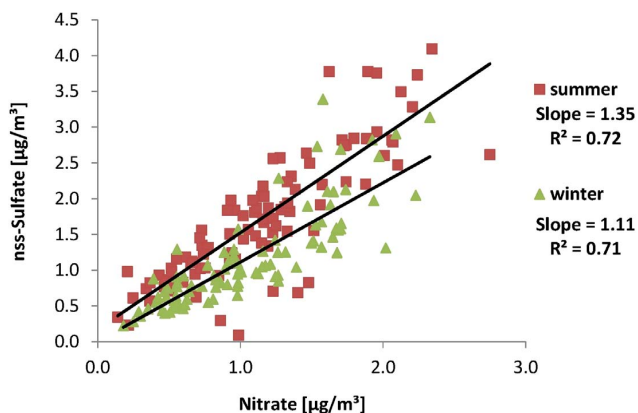


**Figure 5.** Correlation between nitrate and nss-sulfate between summer and winter in samples collected from July 2010 to November 2011.

be transported in higher amounts from the European and African continent during winter.

However, during summer the photochemical production of particle phase nitrate and sulfate is higher. This may therefore lead to the observed increase in the nss-sulfate concentration reflected by the increase in the slope. The combined effects of increased winter emissions of anthropogenic precursors reducing winter and enhancing summer photochemical conversion might explain the effect depicted in Fig. 5. However, further investigations are necessary in order to clearly explain the difference.

### 3.4.2 Nss-sulfate and oxalate

The scatterplot of nss-sulfate and oxalate shows weak correlation between both species during winter and summer. However, the winter correlation (Fig. 6a) was weaker than the summer correlation (Fig. 6b), with a lot of scattering in the data. These correlations were only observed during days with high marine air mass influence and low aerosol mass loading, with negligible influence from anthropogenic emissions. During a period of 11 days with dominant marine-influenced air mass in spring 2011, an even stronger correlation between nss-sulfate and oxalate ( $r^2 = 0.90$ ) was observed (Fig. 6c). This suggests that there is a strong influence of surface water temperatures on oxalate and nss-sulfate concentrations. It can be assumed that the clean air mass was influenced by marine emissions of DMS, ethene and other marine organic precursors and subsequent photochemical aqueous phase reactions might have led to the formation of oxalate (Tilgner and Herrmann, 2010). As mentioned above, high surface water temperatures are known to also influence the production of nss-sulfate. Thus we conclude that both nss-sulfate and oxalate within this period could have originated from different precursors of marine origin, such as from marine organisms – e.g., algae – or from their emissions.

### 3.4.3 Ammonium and chlorophyll *a*

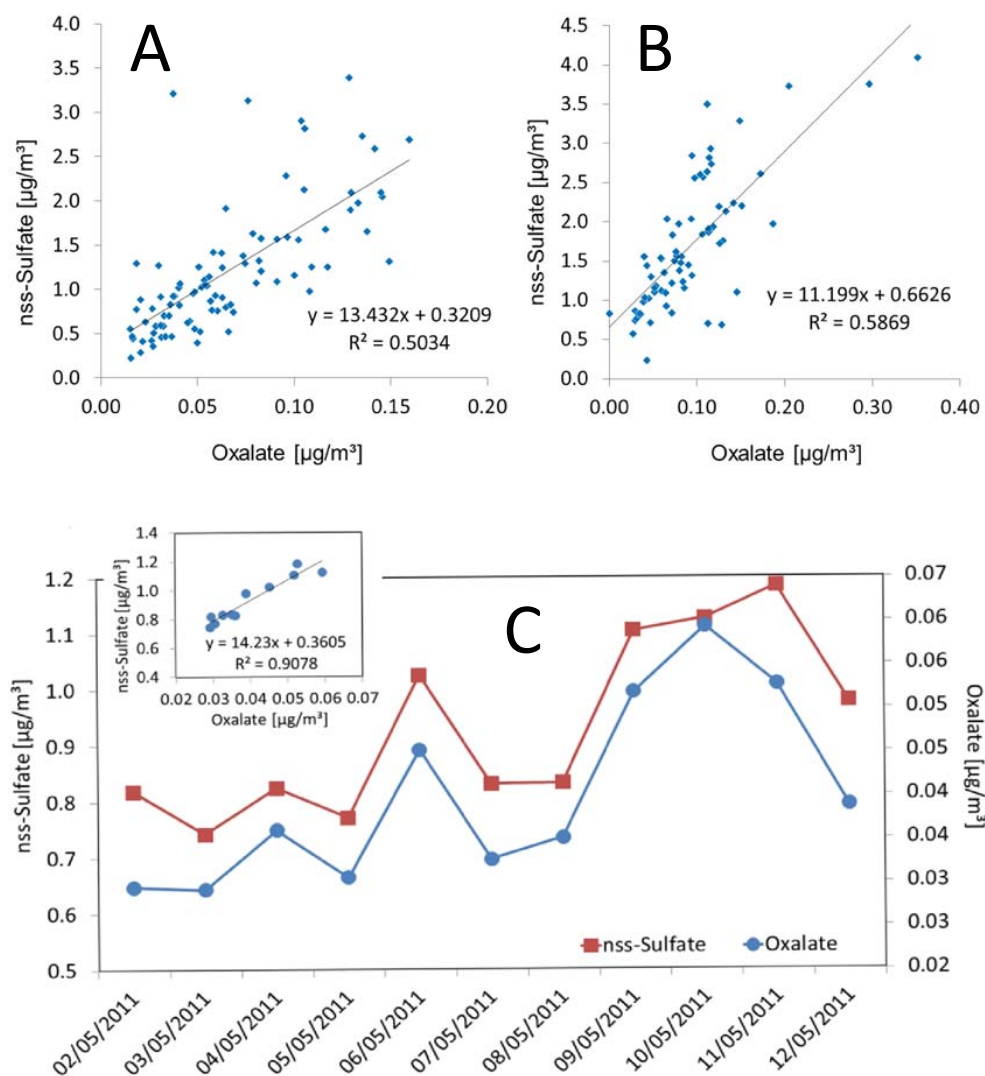
Figure 7 shows the concentration profiles of ammonium, chlorophyll *a* and oxalate. The temporal variability of ammonium and chlorophyll *a* showed similar trends, implying a coincidence of these species. Increase in ammonium concentration was often correlated with an increase in chlorophyll *a* concentration in the ocean's surface. The chlorophyll *a* concentration was taken from monthly averaged MODIS (Moderate-Resolution Imaging Spectroradiometer) Aqua satellite images over a region east and northeast of São Vicente achieved from <http://disc.sci.gsfc.nasa.gov/giovanni/overview/index.html>. The chlorophyll *a* maximum was observed between May and June. Chlorophyll *a* concentrations in the region northeast of Cape Verde are usually higher in spring than in the other seasons, and they are influenced by the delivery of nutrients by higher upwelling intensity (Lathuiliere et al., 2008; Ohde and Siegel, 2010) in the Mauritanian upwelling region. The observed coincidence between ammonium and chlorophyll *a* suggests that the ocean might be a source of ammonium in this region as illustrated above.

A similar correlation between chlorophyll *a* and ammonium has been reported before. Clarke and Porter (1993) found a good correlation between enhanced ammonium aerosol concentrations and enhanced chlorophyll concentrations during an equatorial Pacific Ocean cruise and concluded that the observed ammonia was a result of equatorial upwelling. Jickells et al. (2003) also concluded on the basis of isotopic measurements of ammonium in marine aerosols that the ocean was a possible source of their observed ammonium concentrations in the North and South Atlantic Ocean.

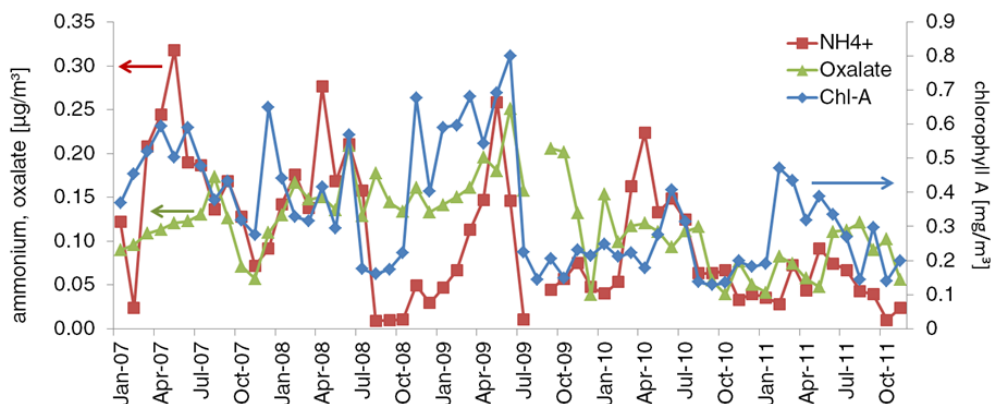
Quinn et al. (1988) also observed ammonia in the remote Pacific Ocean and the atmosphere and concluded that the observed atmospheric ammonium originated from the ocean. Although the ocean is a significant source of ammonia during remote conditions, long-range transport of ammonia or ammonium salts from the African continent or SW Europe were also important sources of ammonia in this region.

### 3.4.4 Elemental carbon (EC) and nss-potassium

A similar temporal variation was observed in the time series of nss-potassium and elemental carbon concentrations during dust events when elevated OC and EC concentrations were observed (Fig. 8) with correlation factor ( $r^2 = 0.6$ ). In principle, this correlation was only observed during about 50 % of the time when air mass inflow was from Africa. Nss-potassium is a known tracer for biomass burning activities. This correlation thereby suggests that biomass burning could partly account for the observed EC concentrations at CVAO, especially during air mass inflow from Africa. However, when the air mass origin was from Europe or from the oceans, no correlation could be observed between nss-potassium and EC.



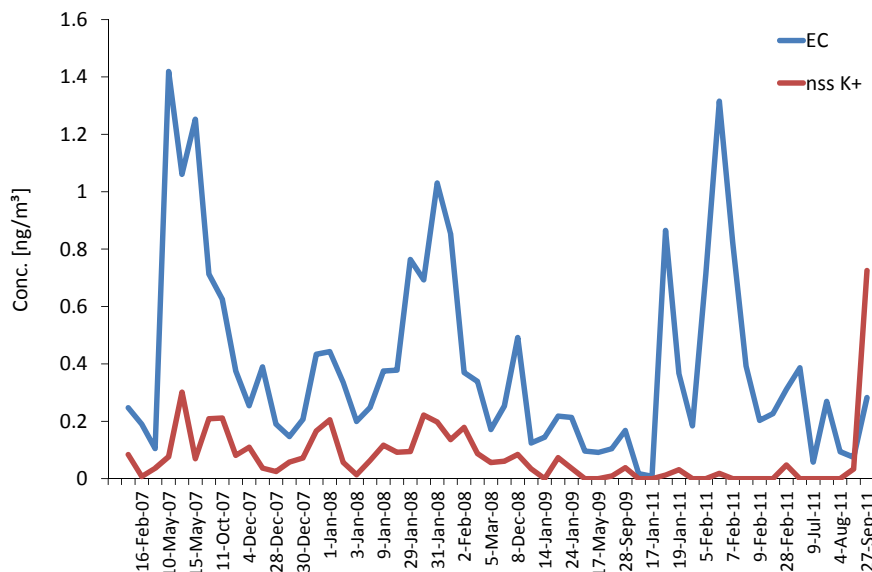
**Figure 6.** Correlation between nss-sulfate and oxalate in filter samples during 2010/2011. Above: (a) winter, (b) summer. Below: (c) concentration and correlation during a marine clean air episode in May 2011.



**Figure 7.** Monthly mean of chlorophyll *a* in the tropical NE Atlantic (selected area for averaging: lat (16.985, 24.895), lon (-24.87, -18.278)), oxalate and ammonium in PM<sub>10</sub> aerosol samples collected at the CVAO.

**Table 5.** Comparison of major non-sea-salt components and halogenide depletion (mean values and standard deviation as an estimation of the scatter) in four classes of particulate matter collected at the tower at the CVAO.

Concentration [ $\mu\text{g m}^{-3}$ ]	Dust-rich Saharan aerosol	Marine aerosol summer	Marine aerosol winter	Europe-influenced aerosol	Mean of all samples
Mass concentration (N)	$173.4 \pm 95.5$ (56)	$16.4 \pm 4.5$ (43)	$14.5 \pm 5.8$ (33)	$35.3 \pm 13.6$ (55)	$47.3 \pm 55.5$ (539)
Dust (estimated)	$144.6 \pm 95.8$	$2.7 \pm 2.6$	$2.0 \pm 4.1$	$6.1 \pm 9.9$	$25.8 \pm 51.4$
OM	$3.16 \pm 1.69$	$0.58 \pm 0.35$	$1.04 \pm 0.7$	$0.86 \pm 0.47$	$1.01 \pm 1.04$
EC	$0.38 \pm 0.32$	$0.05 \pm 0.05$	$0.04 \pm 0.03$	$0.12 \pm 0.08$	$0.13 \pm 0.16$
Nitrate	$1.75 \pm 0.69$	$0.58 \pm 0.28$	$0.48 \pm 0.22$	$1.36 \pm 0.49$	$1.10 \pm 0.56$
Non-sea-salt sulfate	$2.46 \pm 1.05$	$1.01 \pm 0.45$	$0.47 \pm 0.31$	$1.76 \pm 0.99$	$1.54 \pm 1.04$
Ammonium	$0.064 \pm 0.08$	$0.07 \pm 0.05$	$0.036 \pm 0.$	$0.165 \pm 0.18$	$0.088 \pm 0.10$
Time over ocean [h]	< 48	> 120	> 120	> 72	–
Chloride depletion [%]	$8.8 \pm 8.5$	$26 \pm 15$	$20 \pm 13$	$30 \pm 12$	$16 \pm 10$
Bromide depletion [%]	$62 \pm 42$	$88 \pm 13$	$83 \pm 20$	$87 \pm 11$	$80 \pm 20$
$[\text{Cl}^-]/[\text{Na}^+]$ (1.17 in sea water)	1.06	0.95	1.03	0.80	
$[\text{Cl}^- + \text{NO}_3^-]/[\text{Na}^+]$	1.19	1.02	1.10	0.91	

**Figure 8.** Time series of nss-potassium (nss-K<sup>+</sup>) and elemental carbon (EC) measured during air mass inflow from Africa revealing similar temporal variations.

### 3.5 Bromide and chloride depletion in PM<sub>10</sub>

Bromide and chloride deficits indicate significant reactive cycling of halogens and do influence the reactive capacity of the marine environment by release of more reactive chloride to the atmosphere. Bromide and chloride deficits in marine aerosols have been reported in different marine environments (Mozurkewich, 1995; Kerminen et al., 1998; Kumar and Sarin, 2010; Yao and Zhang, 2012). The reported (Liebezeit, 2011) sodium-to-chloride (bromide) mass ratio in sea salt is 0.56 (162.4), and the molar ratio is 0.85 (46.73). The chlo-

ride (bromide) depletion is estimated as the percentage loss in chloride (bromide) from sea salt chloride (bromide) concentrations leading to higher values of the sodium to chloride (bromide) ratios. In the atmosphere, when bromide and chloride react with acidic gases or particles containing nitric, sulfuric or organic acids to form HO<sub>x</sub>, X<sub>2</sub> and other compounds, the evaporation of volatile bromine/chlorine compounds occurs, and bromide and chloride losses are observed in marine aerosols, leading to an increase in the sodium to chloride (bromide) ratio. This effect of bromide/chloride depletion is known to increase with decreasing particle size from about

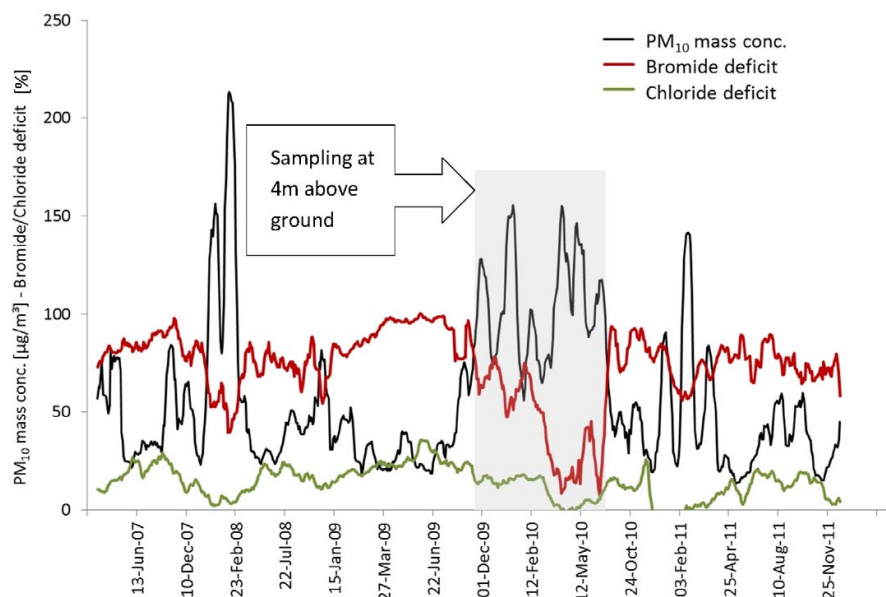


**Figure 9.** Variability of bromide and chloride deficit in comparison to the total  $\text{PM}_{10}$  mass concentration (all curves represent 10 sample running mean) and the season.

30 to 100 % in the presence of anthropogenic pollutants (Hsu et al., 2007; Quinn and Bates, 2005). In this study, bromide and chloride depletion was observed in  $\text{PM}_{10}$  samples and is discussed according to seasons, sampling height and dust concentration.

Figure 9 shows the temporal variation in the chloride/bromide depletion and aerosol mass concentration during 5 years of measurements at CVAO. Bromide loss was always higher than chloride loss, with average bromide and chloride losses of about 80 and 16 %, respectively. Periods of Saharan dust influence observed as peaks in the aerosol mass concentrations usually yielded 62 % bromide and 9 % chloride loss.

At lower sampling height, fresh sea spray particles have shorter residence time in the atmosphere prior to their collection and thus should have insignificant bromide/chloride deficits. However, due to the mixture of aged and long-range-transported aerosols with the freshly emitted marine particles, bromide (chloride) depletion of about 4 % was observed at this height. In Table 5 the average chloride and bromide deficits for the typical air mass inflow of the particles and their precursors are given. Higher halogen depletion was observed during periods of low aerosol mass concentration with less influence of Saharan dust. Long-range-transported and aged sea salt particles lose more chloride (bromide) due to their long atmospheric residence time and thus more time for interaction with acidic compounds. The highest chloride (bromide) loss of about 30 % (87 %) was observed when the air mass crossed southwestern Europe prior to its arrival at CVAO and had relatively long (72 h) residence time over the ocean. The more anthropogenically influenced SW European

particles and gaseous compounds thus had sufficient time to adsorb onto and react with sea salt particles, resulting in a higher exchange and displacement of halogenides from sea salt particles as compared to periods when particles spend less time over the ocean as is the case during Saharan dust events.

The chloride depletion during winter and summer marine air masses (Fig. 1a) was about 5 % lower than the loss observed during SW-Europe-influenced air mass inflow. The air mass origin, aerosol acidic component concentration and the sea salt particle atmospheric lifetime were the determining factors towards the halogenide depletion. The deficits were higher in the summer than in the winter. This was likely due to varying solar irradiation intensity and the concentration difference of the aerosol acidic components of sulfuric and nitric acid in these samples. During marine-influenced air mass inflow the nss-sulfate concentration in the summer was twice as much as that observed in the winter, likely due to the increase in photochemical production activities and the emission of marine nss-sulfate precursors, as previously explained. Thus the additional nss-sulfate source and higher solar irradiation are most probably among the reasons for the increased chloride/bromide loss during the summer in comparison to the winter for marine-influenced air masses.

Nevertheless, although the concentration of nitrate and non-sea salt sulfate was high during Saharan dust events, the chloride/bromide depletion was found to be the lowest. Figure 9 depicts a clear anti-correlation between  $\text{PM}$  mass concentration and halogenide loss. This effect was clearly seen in winter 2007/2008 and 2010/2011. During the winter 2008/2009 the dust events were less intensive, and the winter

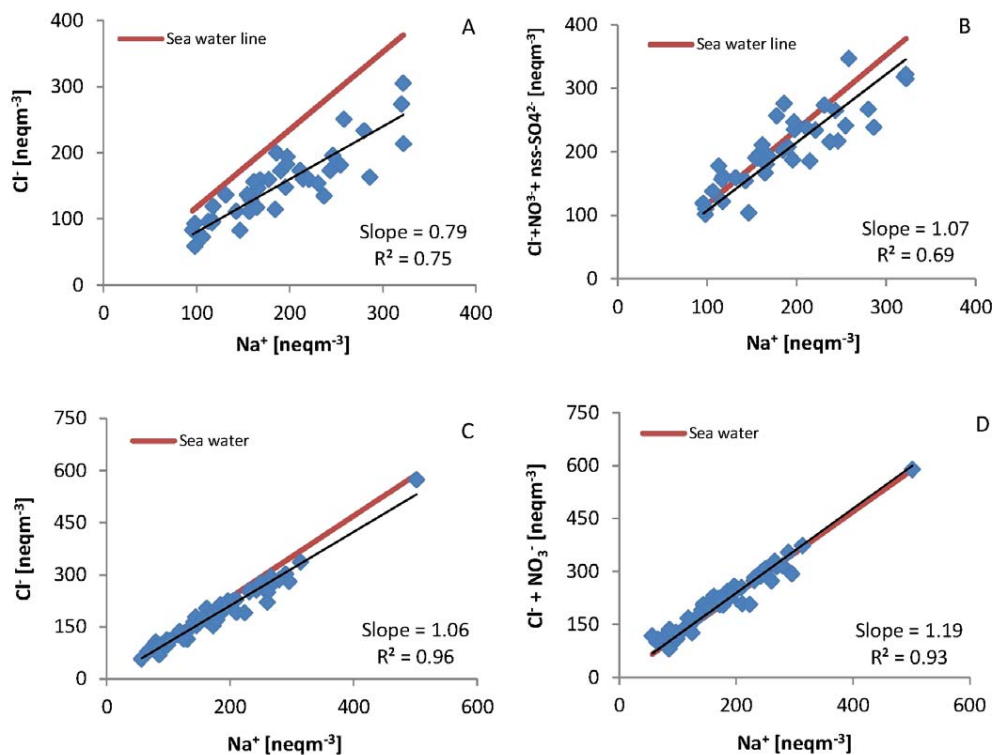


**Figure 10.** Scatterplots between (a)  $\text{Na}^+$  and  $\text{Cl}^-$ , and (b)  $\text{Na}^+$  and  $\text{Cl}^- + \text{NO}_3^- + \text{nss-SO}_4^{2-}$  during summer marine air mass inflow and between (c)  $\text{Na}^+$  and  $\text{Cl}^-$ , and (d)  $\text{Na}^+$  and  $\text{Cl}^- + \text{NO}_3^-$  during Saharan dust events at the CVAO.

sampling period 2009/2010 took place at a lower sampling height with a greater influence of sea spray.

During dust events there is not only an increase in acidic species but also an increase in cations and carbonates. The increase in cations concentration provides additional reactive sites for the acidic species, thus reducing the possibility for the direct reaction on sea salt particles and, therefore, decreasing the overall displacement of halogenides from sodium. Furthermore, gaseous halogenides could react with  $\text{CaCO}_3$ , as shown by Sullivan et al. (2007), leading to a buffering effect of the dust on the sea salt particles and thereby resulting in a more externally mixed aerosol. Thus a combination of low residence time as mentioned above and higher competition of cations sites during dust events leads to a lower effective loss of chloride and bromide from sea salt particles in comparison to the other situations. We thus suggest that in this region of the Atlantic these three processes – photochemistry, air mass residence time and concentration of acidic components – are the determining driving factors towards halogenide deficits in the observed aerosol.

### 3.5.1 Contribution of acidic species to chloride depletion

The most important aerosol acidic species are nitric and sulfuric acids since their concentrations are far higher than those

of other acidic species, such as oxalic acid (in non-dusty aerosol). As explained above, the highest chloride deficit was observed when air mass inflow was from Europe. The scatterplot of equivalent concentrations of  $\text{Na}^+$  and  $\text{Cl}^-$  (Fig. 10a) shows that the data points fall below the theoretical values in sea water and only approaches this line when the  $\text{Cl}^-$  concentration is matched with nitrate and nss-sulfate concentrations (Fig. 10b). Thus, assuming all available nitrate and nss-sulfate species were involved in chloride depletion, this would account only for about 90 % of the chloride depletion. The actual contribution of these species is, however, much less since they may also be associated with  $\text{NH}_4^+$ , nss- $\text{K}^+$  or  $\text{Ca}^{2+}$ , which are possible neutralizers of the available nitric and sulfuric acids. Thus, considering the neutralization of sulfuric or nitric acid by ammonium or other cations, the excess sulfuric or nitric acid available will be even less and they would thus account for less than 90 % of the chloride depletion. This indicates that during air mass inflow from Europe other process mechanisms different from acid displacement reactions, such as photochemical reactions with ozone or NO (Behnke and Zetzsch, 1990), could have been involved in chloride depletion.

A similar tendency was observed in samples where air mass inflow was of marine origin during the summer. The estimated chloride loss was about 26 %, and the concentrations of the acidic components were also elevated, but the

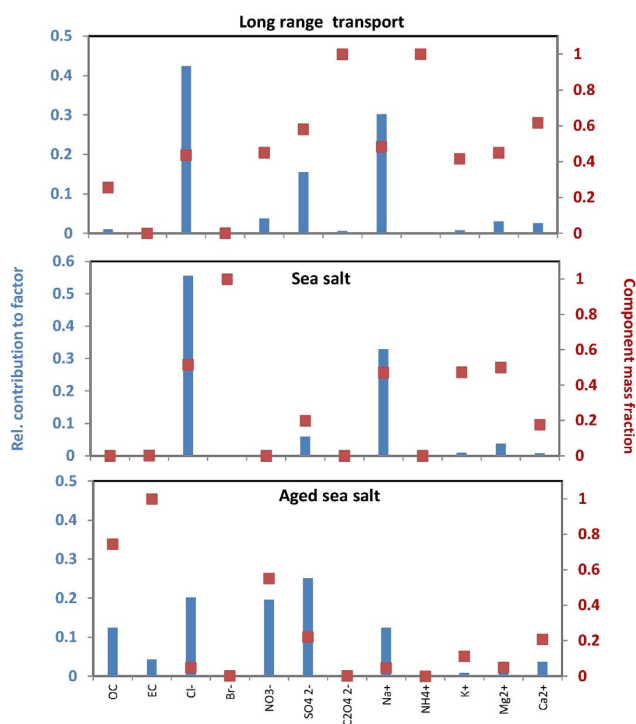


**Figure 11.** Source profiles identified from measured PM<sub>10</sub> components at CVAO. Results are from 671 analyzed filters. The relative contribution of each species to a given factor is represented by blue bars, while the relative contribution of each factor to the total species concentration is represented by a red square (right axis).

acid displacement of neither nitric nor sulfuric acids was sufficient to account for the chloride loss. Their contribution, however, could only explain about 95 % of the chloride loss, assuming these species were not associated with other cations. The only situation whereby acidic species could sufficiently account for chloride loss was during Saharan dust events as shown in Fig. 10c and d. The scatterplot shows good correlation slightly above the theoretical sea water line for Na<sup>+</sup> and Cl<sup>-</sup> when Cl<sup>-</sup> concentrations are marched with NO<sub>3</sub><sup>-</sup>, indicating that, within error margins, nitric acid displacement was the main reaction leading to chloride loss during dust events. This claim is supported by results of size-resolved distribution of aerosol components previously reported by Müller et al. (2010) which showed that during dust events about 90 % of nitrate is found in the coarse mode together with sea salt particles, while nss-sulfate concentration are concentrated in the fine mode. Thus in all non-Saharan-dust-influenced days at CVAO, photochemistry was a determining factor towards chloride loss; while during dust events, nitric acid played the major role.

### 3.6 PMF source apportionment analysis

The PMF analysis was applied to identify the possible sources of the aerosol observed at the CVAO during the

investigated time period. The chemical composition matrix was made of the 12 analyzed chemical species (water-soluble ions, OC and EC). Three major sources were identified by having clear different signatures as fresh sea salt, aged sea salt and long-range transport. Figure 11 shows the source profiles (blue bars) and the relative contribution of each factor to the total species concentration in the samples (red squares). There was no ideal tracer for mineral dust since trace metal analysis were not performed on these filters. However, due to the strong correlation between nss-Ca<sup>2+</sup> and Ca<sup>2+</sup> during dust storms ( $r^2 = 0.99$ ), calcium occurrence was considered as a possible indicator of mineral dust or long-range-transported dust particles. The fresh sea salt factor was characterized by similar (Liebezeit, 2011) sea water proportions of Na (35 %), Cl (54 %), sulfate (7 %) and magnesium (4 %). The model-obtained fractions were quite similar to reported sea water concentration and indicated that PMF is a useful tool in identifying sources in complex aerosol samples. In principle, this factor represents freshly emitted sea salt particles due to the strong agreement with sea water proportions and the little association with non-sea salt species. Thus, freshly emitted sea salt particles dominated the ionic composition of the aerosol as it made up about 50 % of its ionic and organic matter content (Fig. 12). This factor could account for the total bromide and 50 % of chloride, sodium, potassium and magnesium concentrations in the samples.

The aged sea salt source was the second-most-important source, making up about 36 % of the total ionic and organic mass. It was characterized by elevated sulfate (14 %), nitrate (6 %) and OC (4 %) concentrations associated with sea salt particles. This source describes sea salt particles that interact with acidic gases or marine emitted organic matter, such as SOA and nss-sulfate from DMS chemistry. The lower chloride (42 %) to sodium (31 %) ratio in this factor is a strong indication of chloride loss due to one of the processes mentioned above. As has also been reported in other works (Amato et al., 2009), sulfate and nitrate association with sea salt particles in this work was also considered as an indicator of the aged sea salt source. This source could account for about 62 % of the total observed soluble calcium, 58 % of the sulfate, 45 % of the nitrate and 25 % of the organic matter observed in the samples.

Finally, the long-range transport factor was characterized by calcium, organic and elemental carbon as well as elevated sulfate and nitrate concentrations. This factor could explain 14 % of the source of the investigated ionic and organic components. The unique tracer for this factor was the presence of EC. EC as well as OC can originate from traffic emissions, biomass burning or ship emissions. Emitted particles from such anthropogenic activities may only reach the CVAO via long-range transport. This factor could account for the presence of all EC, 80 % of the OC and 60 % of the nitrate observed at the CVAO. A comparison of this factor with our Saharan dust estimation showed most of the time a similar time

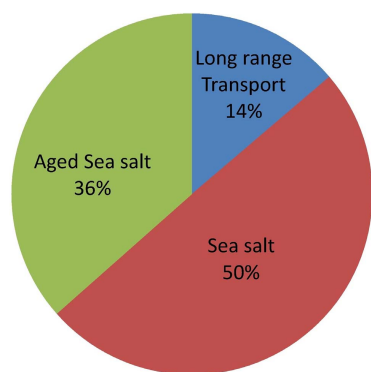


**Figure 12.** Average contribution of each source to the total analyzed species.

series. Therefore, the estimated mineral dust profile could be explained by the long-range transport source.

Although the PMF model could not successfully separate mineral dust and long-range-transported particles due to the limited data input, the obtained results are still representative of this region of the Atlantic, are unique and show that mineral dust contributes not more than 14 % of the water-soluble ions and organic mass budget at CVAO.

#### 4 Conclusions

Saharan dust and sea salt dominate the PM<sub>10</sub> particle composition in near-surface air masses at the CVAO. At the standard collection height of 32 m at the CVAO, the long-term mean of sea salt and total PM<sub>10</sub> aerosol were 11 and 47 μg m<sup>-2</sup>, respectively, of which Saharan dust made up 55 % of the PM<sub>10</sub> mass. Secondary ionic species, elemental carbon, organic matter and water completed the particle composition. Seasonal variations were found for aerosol mass, dust, nss-sulfate, EC, OM and ammonium. Ammonium and oxalate were often correlated with chlorophyll *a*, which suggests that ammonia and oxalic acid also had marine precursors in this environment. A distinct seasonality was observed for the halogenide depletion, with the minimum in winter due to the occurrence of Saharan dust events and the lower irradiation intensity in non-dust periods. Chloride depletion varied between 10 and 35 %. In marine air masses during the summer and in polluted air masses from SW Europe, bromide was often fully depleted, while chloride observed its highest depletions. Photochemistry, air mass residence time and concentration of acidic components were the main factors controlling halogenide depletion in this region. While photochemistry was decisive during summer, nitric acid played a major role towards chloride depletion during dust storms.

Ground-based long-term investigation of PM at the CVAO is an important step towards understanding the role of aerosols in ocean–atmosphere interactions especially in the eastern tropical North Atlantic. The observed strong annual

and seasonal variation of the aerosol constitution provides useful information on the type of atmospheric nutrient deposition and how the ocean has responded to this deposition over the past 5 years. Such investigations are quite useful since they provide the relevant background knowledge for understanding in the long term the role the atmosphere and the ocean play in the global climate. Such long-term observations are highly encouraged and would be essential in initializing model runs that can then in more detail describe the link between the atmosphere–ocean interaction and the global climate. Air mass origins with dust source regions and oceanic and meteorological influences during air mass transport must be further investigated to understand their effects on the global climate.

**The Supplement related to this article is available online at doi:10.5194/acp-14-8883-2014-supplement.**

*Acknowledgements.* The efforts of Luis Mendes and Helder Timas Nascimento in sampling and maintenance activities at the CVAO and of the TROPOS laboratory assistants for their helpful work are greatly appreciated. The study was supported by the German BMBF within the SOPRAN I and II projects (FKZ: 03F0462J and 03F0611J) and the EU specific Support Action TENATSO (37090).

Edited by: T. Petäjä

#### References

- Alastuey, A., Querol, X., Castillo, S., Escudero, M., Avila, A., Cuevas, E., Torres, C., Romero, P. M., Exposito, F., Garcia, O., Diaz, J. P., Van Dingenen, R., and Putaud, J. P.: Characterisation of TSP and PM<sub>2.5</sub> at Izana and Sta. Cruz de Tenerife (Canary Islands, Spain) during a Saharan dust episode (July 2002), *Atmos. Environ.*, 39, 4715–4728, doi:10.1016/j.atmosenv.2005.04.018, 2005.
- Allan, J. D., Topping, D. O., Good, N., Irwin, M., Flynn, M., Williams, P. I., Coe, H., Baker, A. R., Martino, M., Niedermeier, N., Wiedensohler, A., Lehmann, S., Müller, K., Herrmann, H., and McFiggans, G.: Composition and properties of atmospheric particles in the eastern Atlantic and impacts on gas phase uptake rates, *Atmos. Chem. Phys.*, 9, 9299–9314, doi:10.5194/acp-9-9299-2009, 2009.
- Alves, C., Oliveira, T., Pio, C., Silvestre, A. J. D., Fialho, P., Barata, F., and Legrand, M.: Characterisation of carbonaceous aerosols from the Azorean Island of Terceira, *Atmos. Environ.*, 41, 1359–1373, doi:10.1016/j.atmosenv.2006.10.022, 2007.
- Amato, F., Pandolfi, M., Escrig, A., Querol, X., Alastuey, A., Pey, J., Perez, N., and Hopke, P. K.: Quantifying road dust resuspension in urban environment by Multilinear Engine: A comparison with PMF2, *Atmos. Environ.*, 43, 2770–2780, doi:10.1016/j.atmosenv.2009.02.039, 2009.
- Angelova, M. D.: Whitecaps, sea-salt aerosols, and climate, Ph.D. dissertation, University of Delaware, 2002.

- Bates, T. S., Lamb, B. K., Guenther, A., Dignon, J., and Stoiber, R. E.: Sulfur emissions to the atmosphere from natural sources, *J. Atmos. Chem.*, 14, 315–337, 1992.
- Bates, T. S., Quinn, P. K., Coffman, D. J., Johnson, J. E., Miller, T. L., Covert, D. S., Wiedensohler, A., Leinert, S., Nowak, A., and Neusüss, C.: Regional physical and chemical properties of the marine boundary layer aerosol across the Atlantic during Aerosols99: An overview, *J. Geophys. Res.-Atmos.*, 106, 20767–20782, 2001.
- Behnke, W. and Zetzsch, C.: Heterogeneous photochemical formation of Cl-atoms from NaCl aerosol, NO<sub>x</sub> and ozone, *J. Aerosol Sci.*, 21, S229–S232, doi:10.1016/0021-8502(90)90226-N, 1990.
- Canonaco, F., Crippa, M., Slowik, J. G., Baltensperger, U., and Prévôt, A. S. H.: SoFi, an IGOR-based interface for the efficient use of the generalized multilinear engine (ME-2) for the source apportionment: ME-2 application to aerosol mass spectrometer data, *Atmos. Meas. Tech.*, 6, 3649–3661, doi:10.5194/amt-6-3649-2013, 2013.
- Carlton, A. G., Turpin, B. J., Altieri, K. E., Seitzinger, S., Reff, A., Lim, H. J., and Ervens, B.: Atmospheric oxalic acid and SOA production from glyoxal: Results of aqueous photooxidation experiments, *Atmos. Environ.*, 41, 7588–7602, doi:10.1016/j.atmosenv.2007.05.035, 2007.
- Carpenter, E. J., Subramaniam, A., and Capone, D. G.: Biomass and primary productivity of the cyanobacterium *Trichodesmium* spp. in the tropical N Atlantic ocean, *Deep-Sea Res. Pt. I*, 51, 173–203, doi:10.1016/j.dsr.2003.10.006, 2004.
- Carpenter, L. J., Fleming, Z. L., Read, K. A., Lee, J. D., Moller, S. J., Hopkins, J. R., Purvis, R. M., Lewis, A. C., Müller, K., Heinold, B., Herrmann, H., Fomba, K. W., van Pinxteren, D., Müller, C., Tegen, I., Wiedensohler, A., Müller, T., Niedermeier, N., Achterberg, E. P., Patey, M. D., Kozlova, E. A., Heimann, M., Heard, D. E., Plane, J. M. C., Mahajan, A., Oetjen, H., Ingham, T., Stone, D., Whalley, L. K., Evans, M. J., Pilling, M. J., Leigh, R. J., Monks, P. S., Karunaharan, A., Vaughan, S., Arnold, S. R., Tschritter, J., Pöhler, D., Friess, U., Holla, R., Mendes, L. M., Lopez, H., Faria, B., Manning, A. J., and Wallace, D. W. R.: Seasonal characteristics of tropical marine boundary layer air measured at the Cape Verde Atmospheric Observatory, *J. Atmos. Chem.*, 67, 87–140, doi:10.1007/s10874-011-9206-1, 2010.
- Chen, Y. and Siefert, R. L.: Determination of various types of labile atmospheric iron over remote oceans, *J. Geophys. Res.-Atmos.*, 108, 4774, doi:10.1029/2003JD003515, 2003.
- Chen, Y. and Siefert, R. L.: Seasonal and spatial distributions and dry deposition fluxes of atmospheric total and labile iron over the tropical and subtropical North Atlantic Ocean, *J. Geophys. Res.-Atmos.*, 109, D09305, doi:10.1029/2003JD003958, 2004.
- Chiapello, I., Bergametti, G., Gomes, L., Chatenet, B., Dulac, F., Pimenta, J., and Soares, E. S.: An additional low layer transport of Sahelian and Saharan dust over the northeastern tropical Atlantic, *Geophys. Res. Lett.*, 22, 3191–3194, doi:10.1029/95gl03313, 1995.
- Chiapello, I., Prospero, J. M., Herman, J. R., and Hsu, N. C.: Detection of mineral dust over the North Atlantic Ocean and Africa with the Nimbus 7 TOMS, *J. Geophys. Res.-Atmos.*, 104, 9277–9291, 1999.
- Clarke, A. D. and Porter, J. N.: Pacific marine aerosol .2. Equatorial gradients in chlorophyll, ammonium, and excess sulfate during Saga-3, *J. Geophys. Res.-Atmos.*, 98, 16997–17010, 1993.
- Clegg, S. L., Brimblecombe, P., and Wexler, A. S.: Thermodynamic model of the system H<sup>+</sup>-NH<sub>4</sub><sup>+</sup>-Na<sup>+</sup>-SO<sub>4</sub><sup>2-</sup>-NB<sub>3</sub><sup>-</sup>-Cl<sup>-</sup>-H<sub>2</sub>O at 298.15 K, *J. Phys. Chem. A*, 102, 2155–2171, doi:10.1021/Jp973043j, 1998.
- Cropp, R. A., Gabric, A. J., McTainsh, G. H., Braddock, R. D., and Tindale, N.: Coupling between ocean biota and atmospheric aerosols: Dust, dimethylsulphide, or artifact?, *Global Biogeochem. Cy.*, 19, GB4002, doi:10.1029/2004GB002436, 2005.
- Facchini, M. C., Decesari, S., Rinaldi, M., Carbone, C., Finessi, E., Mircea, M., Fuzzi, S., Moretti, F., Tagliavini, E., Ceburnis, D., and O'Dowd, C. D.: Important source of marine secondary organic aerosol from biogenic amines, *Environ. Sci. Technol.*, 42, 9116–9121, doi:10.1021/Es8018385, 2008.
- Facchini, M. C., Decesari, S., Rinaldi, M., Finessi, E., Ceburnis, D., O'Dowd, C. D., and Stephanou, E. G.: Marine SOA: Gas-to-particle conversion and oxidation of primary organic aerosol, *Geochim. Cosmochim. Ac.*, 74, A275–A275, 2010.
- Fomba, K. W., Müller, K., van Pinxteren, D., and Herrmann, H.: Aerosol size-resolved trace metal composition in remote northern tropical Atlantic marine environment: case study Cape Verde islands, *Atmos. Chem. Phys.*, 13, 4801–4814, doi:10.5194/acp-13-4801-2013, 2013.
- Formenti, P., Elbert, W., Maenhaut, W., Haywood, J., and Andreae, M. O.: Chemical composition of mineral dust aerosol during the Saharan Dust Experiment (SHADE) airborne campaign in the Cape Verde region, September 2000, *J. Geophys. Res.-Atmos.*, 108, 8576, doi:10.1029/2002jd002648, 2003.
- Formenti, P., Schutz, L., Balkanski, Y., Desboeufs, K., Ebert, M., Kandler, K., Petzold, A., Scheuven, D., Weinbruch, S., and Zhang, D.: Recent progress in understanding physical and chemical properties of African and Asian mineral dust, *Atmos. Chem. Phys.*, 11, 8231–8256, doi:10.5194/acp-11-8231-2011, 2011.
- Ganor, E., Foner, H. A., Bingemer, H. G., Udusti, R., and Setter, I.: Biogenic sulphate generation in the Mediterranean Sea and its contribution to the sulphate anomaly in the aerosol over Israel and the Eastern Mediterranean, *Atmos. Environ.*, 34, 3453–3462, 2000.
- Gantt, B. and Meskhidze, N.: The physical and chemical characteristics of marine primary organic aerosol: a review, *Atmos. Chem. Phys.*, 13, 3979–3996, doi:10.5194/acp-13-3979-2013, 2013.
- Gantt, B., Meskhidze, N., Facchini, M. C., Rinaldi, M., Ceburnis, D., and O'Dowd, C. D.: Wind speed dependent size-resolved parameterization for the organic mass fraction of sea spray aerosol, *Atmos. Chem. Phys.*, 11, 8777–8790, doi:10.5194/acp-11-8777-2011, 2011.
- Gelado-Caballero, M. D., Lopez-Garcia, P., Prieto, S., Patey, M. D., Collado, C., and Hernandez-Brito, J. J.: Long-term aerosol measurements in Gran Canaria, Canary Islands: Particle concentration, sources and elemental composition, *J. Geophys. Res.-Atmos.*, 117, D03304, doi:10.1029/2011jd016646, 2012.
- Gnauk, T., Müller, K., van Pinxteren, D., He, L. Y., Niu, Y. W., Hu, M., and Herrmann, H.: Size-segregated particulate chemical composition in Xinken, Pearl River Delta, China: OC/EC and organic compounds, *Atmos. Environ.*, 42, 6296–6309, doi:10.1016/j.atmosenv.2008.05.001, 2008.

- Harrison, R. M., Jones, A. M., and Lawrence, R. G.: A pragmatic mass closure model for airborne particulate matter at urban background and roadside sites, *Atmos. Environ.*, 37, 4927–4933, doi:10.1016/j.atmosenv.2003.08.025, 2003.
- Heller, M. I. and Croot, P. L.: Superoxide decay as a probe for speciation changes during dust dissolution in Tropical Atlantic surface waters near Cape Verde, *Mar. Chem.*, 126, 37–55, doi:10.1016/j.marchem.2011.03.006, 2011.
- Hsu, S. C., Liu, S. C., Kao, S. J., Jeng, W. L., Huang, Y. T., Tseng, C. M., Tsai, F., Tu, J. Y., and Yang, Y.: Water-soluble species in the marine aerosol from the northern South China Sea: High chloride depletion related to air pollution, *J. Geophys. Res.-Atmos.*, 112, D19304, doi:10.1029/2007jd008844, 2007.
- Jaenicke, R.: Atmospheric aerosols and global climate, *J. Aerosol Sci.*, 11, 577–588, doi:10.1016/0021-8502(80)90131-7, 1980.
- Jickells, T. D., Kelly, S. D., Baker, A. R., Biswas, K., Dennis, P. F., Spokes, L. J., Witt, M., and Yeatman, S. G.: Isotopic evidence for a marine ammonia source, *Geophys. Res. Lett.*, 30, 1374, doi:10.1029/2002GL016728, 2003.
- Johansen, A. M., Siefert, R. L., and Hoffmann, M. R.: Chemical composition of aerosols collected over the tropical North Atlantic Ocean, *J. Geophys. Res.-Atmos.*, 105, 15277–15312, doi:10.1029/2000jd900024, 2000.
- Kandler, K., Benker, N., Bundke, U., Cuevas, E., Ebert, M., Knippertz, P., Rodriguez, S., Schutz, L., and Weinbruch, S.: Chemical composition and complex refractive index of Saharan mineral dust at Izana, Tenerife (Spain) derived by electron microscopy, *Atmos. Environ.*, 41, 8058–8074, doi:10.1016/j.atmosenv.2007.06.047, 2007.
- Kandler, K., Lieke, K., Benker, N., Emmel, C., Kupper, M., Müller-Ebert, D., Ebert, M., Scheuven, D., Schladitz, A., Schutz, L., Weinbruch, S.: Electron microscopy of particles collected at Praia, Cape Verde, during the Saharan Mineral Dust Experiment: particle chemistry, shape, mixing state and complex refractive index, *Tellus B* 63, 475–496, 2011.
- Kawamura, K. and Gagosian, R. B.: Implications of omega-oxocarboxylic acids in the remote marine atmosphere for photooxidation of unsaturated fatty-acids, *Nature*, 325, 330–332, 1987.
- Kawamura, K. and Sakaguchi, F.: Molecular distributions of water soluble dicarboxylic acids in marine aerosols over the Pacific Ocean including tropics, *J. Geophys. Res.-Atmos.*, 104, 3501–3509, doi:10.1029/1998jd100041, 1999.
- Kelly, J. T., Chuang, C. C., and Wexler, A. S.: Influence of dust composition on cloud droplet formation, *Atmos. Environ.*, 41, 2904–2916, doi:10.1016/j.atmosenv.2006.12.008, 2007.
- Kerminen, V. M., Teinila, K., Hillamo, R., and Pakkanen, T.: Substitution of chloride in sea-salt particles by inorganic and organic anions, *J. Aerosol Sci.*, 29, 929–942, 1998.
- Kettle, A. J., Andreae, M. O., Amouroux, D., Andreae, T. W., Bates, T. S., Berresheim, H., Bingemer, H., Boniforti, R., Curran, M. A. J., DiTullio, G. R., Helas, G., Jones, G. B., Keller, M. D., Kiene, R. P., Leck, C., Lévassieur, M., Malin, G., Maspero, M., Matrai, P., McTaggart, A. R., Mihalopoulos, N., Nguyen, B. C., Novo, A., Putaud, J. P., Rapsomanikis, S., Roberts, G., Schebeske, G., Sharma, S., Simo, R., Staubes, R., Turner, S., and Uher, G.: A global database of sea surface dimethylsulfide (DMS) measurements and a procedure to predict sea surface DMS as a function of latitude, longitude, and month, *Global Biogeochem. Cy.*, 13, 399–444, 1999.
- Kouvarakis, G. and Mihalopoulos, N.: Seasonal variation of dimethylsulfide in the gas phase and of methanesulfonate and non-sea-salt sulfate in the aerosols phase in the Eastern Mediterranean atmosphere, *Atmos. Environ.*, 36, 929–938, 2002.
- Kumar, A., and Sarin, M. M.: Atmospheric water-soluble constituents in fine and coarse mode aerosols from high-altitude site in western India: Long-range transport and seasonal variability, *Atmos. Environ.*, 44, 1245–1254, doi:10.1016/j.atmosenv.2009.12.035, 2010.
- Lathuiliere, C., Echevin, V., and Levy, M.: Seasonal and intraseasonal surface chlorophyll-a variability along the north-west African coast, *J. Geophys. Res.-Oceans*, 113, C05007, doi:10.1029/2007jc004433, 2008.
- Lee, J. D., McFiggans, G., Allan, J. D., Baker, A. R., Ball, S. M., Benton, A. K., Carpenter, L. J., Commane, R., Finley, B. D., Evans, M., Fuentes, E., Furneaux, K., Goddard, A., Good, N., Hamilton, J. F., Heard, D. E., Herrmann, H., Hollingsworth, A., Hopkins, J. R., Ingham, T., Irwin, M., Jones, C. E., Jones, R. L., Keene, W. C., Lawler, M. J., Lehmann, S., Lewis, A. C., Long, M. S., Mahajan, A., Methven, J., Moller, S. J., Müller, K., Müller, T., Niedermeier, N., O'Doherty, S., Oetjen, H., Plane, J. M. C., Pszenny, A. A. P., Read, K. A., Saiz-Lopez, A., Saltzman, E. S., Sander, R., von Glasow, R., Whalley, L., Wiedensohler, A., and Young, D.: Reactive Halogens in the Marine Boundary Layer (RHAMBLE): the tropical North Atlantic experiments, *Atmos. Chem. Phys.*, 10, 1031–1055, doi:10.5194/acp-10-1031-2010, 2010.
- Liebezeit, G.: Meereschemie und globaler Wandel. In: Warnsignal Klima - Die Meere – Änderungen & Risiken, edited by: Lozán, J. L., Graßl, H., Karbe, L., and Reise, K., Wissenschaftliche Auswertungen, Hamburg, p. 32, 2011.
- Mahajan, A. S., Plane, J. M. C., Oetjen, H., Mendes, L., Saunders, R. W., Saiz-Lopez, A., Jones, C. E., Carpenter, L. J., and McFiggans, G. B.: Measurement and modelling of tropospheric reactive halogen species over the tropical Atlantic Ocean, *Atmos. Chem. Phys.*, 10, 4611–4624, doi:10.5194/acp-10-4611-2010, 2010.
- Mahowald, N. M., Baker, A. R., Bergametti, G., Brooks, N., Duce, R. A., Jickells, T. D., Kubilay, N., Prospero, J. M., and Tegen, I.: Atmospheric global dust cycle and iron inputs to the ocean, *Global Biogeochem. Cy.*, 19, GB4025, doi:10.1029/2004gb002402, 2005.
- Mihalopoulos, N., Stephanou, E., Kanakidou, M., Pilitsidis, S., and Bousquet, P.: Tropospheric aerosol ionic composition in the Eastern Mediterranean region, *Tellus B*, 49, 314–326, 1997.
- Milton, S. F., Greed, G., Brooks, M. E., Haywood, J., Johnson, B., Allan, R. P., Slingo, A., and Grey, W. M. F.: Modeled and observed atmospheric radiation balance during the West African dry season: Role of mineral dust, biomass burning aerosol, and surface albedo, *J. Geophys. Res.-Atmos.*, 113, D00C02, doi:10.1029/2007JD009741, 2008.
- Mozurkewich, M.: Mechanisms for the release of halogens from sea-salt particles by free-radical reactions, *J. Geophys. Res.-Atmos.*, 100, 14199–14207, doi:10.1029/94JD00358, 1995.
- Müller, C., Iinuma, Y., Karstensen, J., van Pinxteren, D., Lehmann, S., Gnauk, T., and Herrmann, H.: Seasonal variation of aliphatic amines in marine sub-micrometer particles at the Cape Verde is-

- lands, *Atmos. Chem. Phys.*, 9, 9587–9597, doi:10.5194/acp-9-9587-2009, 2009.
- Müller, K., Lehmann, S., van Pinxteren, D., Gnauk, T., Niedermeier, N., Wiedensohler, A., and Herrmann, H.: Particle characterization at the Cape Verde atmospheric observatory during the 2007 RHaMBLe intensive, *Atmos. Chem. Phys.*, 10, 2709–2721, doi:10.5194/acp-10-2709-2010, 2010.
- Neusüss, C., Wex, H., Birmili, W., Wiedensohler, A., Koziar, C., Busch, B., Brüggemann, E., Gnauk, T., Ebert, M., and Covert, D. S.: Characterization and parameterization of atmospheric particle number-, mass-, and chemical-size distributions in central Europe during LACE 98 and MINT, *J. Geophys. Res.-Atmos.*, 107, 8127, doi:10.1029/2001jd000514, 2002.
- Niedermeier, N., Held, A., Müller, T., Heinold, B., Schepanski, K., Tegen, I., Kandler, K., Ebert, M., Weinbruch, S., Read, K., Lee, J., Fomba, K. W., Müller, K., Herrmann, H., and Wiedensohler, A.: Mass deposition fluxes of Saharan mineral dust to the tropical northeast Atlantic Ocean: an intercomparison of methods, *Atmos. Chem. Phys.*, 14, 2245–2266, doi:10.5194/acp-14-2245-2014, 2014.
- O'Dowd, C. D. and De Leeuw, G.: Marine aerosol production: a review of the current knowledge, *Philos. T. R. Soc. A*, 365, 1753–1774, doi:10.1098/rsta.2007.2043, 2007.
- O'Dowd, C. D., Facchini, M. C., Cavalli, F., Ceburnis, D., Mircea, M., Decesari, S., Fuzzi, S., Yoon, Y. J., and Putaud, J. P.: Biogenically driven organic contribution to marine aerosol, *Nature*, 431, 676–680, doi:10.1038/Nature02959, 2004.
- Ohde, T. and Siegel, H.: Biological response to coastal upwelling and dust deposition in the area off Northwest Africa, *Cont. Shelf Res.*, 30, 1108–1119, doi:10.1016/j.csr.2010.02.016, 2010.
- Paatero, P.: The multilinear engine – A table-driven, least squares program for solving multilinear problems, including the n-way parallel factor analysis model, *J. Comp. Graph. Stat.*, 8, 854–888, doi:10.2307/1390831, 1999.
- Pavuluri, C. M., Kawamura, K., Kikuta, M., Tachibana, E., and Agarwal, S. G.: Time-resolved variations in the distributions of inorganic ions, carbonaceous components, dicarboxylic acids and related compounds in atmospheric aerosols from Sapporo, northern Japan during summertime, *Atmos. Environ.*, 62, 622–630, doi:10.1016/j.atmosenv.2012.08.063, 2012.
- Quinn, P. K. and Bates, T. S.: Regional aerosol properties: Comparisons of boundary layer measurements from ACE 1, ACE 2, aerosols99, INDOEX, ACE asia, TARFOX, and NEAQS, *J. Geophys. Res.-Atmos.*, 110, D14202, doi:10.1029/2004JD004755, 2005.
- Quinn, P. K., Charlson, R. J., and Bates, T. S.: Simultaneous observations of ammonia in the atmosphere and ocean, *Nature*, 335, 336–338, doi:10.1038/335336a0, 1988.
- Radhi, M., Box, M. A., Box, G. P., Mitchell, R. M., Cohen, D. D., Stelcer, E., and Keywood, M. D.: Optical, physical and chemical characteristics of Australian continental aerosols: results from a field experiment, *Atmos. Chem. Phys.*, 10, 5925–5942, doi:10.5194/acp-10-5925-2010, 2010.
- Raes, F., Liao, H., Chen, W. T., and Seinfeld, J. H.: Atmospheric chemistry-climate feedbacks, *J. Geophys. Res.-Atmos.*, 115, D12121, doi:10.1029/2009JD013300, 2010.
- Read, K. A., Mahajan, A. S., Carpenter, L. J., Evans, M. J., Faria, B. V. E., Heard, D. E., Hopkins, J. R., Lee, J. D., Moller, S. J., Lewis, A. C., Mendes, L., McQuaid, J. B., Oetjen, H., Saiz-Lopez, A., Pilling, M. J., and Plane, J. M. C.: Extensive halogen-mediated ozone destruction over the tropical Atlantic Ocean, *Nature*, 453, 1232–1235, doi:10.1038/Nature07035, 2008.
- Reid, E. A., Reid, J. S., Meier, M. M., Dunlap, M. R., Cliff, S. S., Broumas, A., Perry, K., and Maring, H.: Characterization of African dust transported to Puerto Rico by individual particle and size segregated bulk analysis, *J. Geophys. Res.-Atmos.*, 108, 8591, doi:10.1029/2002jd002935, 2003.
- Rijkenberg, M. J. A., Powell, C. F., Dall'Osto, M., Nielsdottir, M. C., Patey, M. D., Hill, P. G., Baker, A. R., Jickells, T. D., Harrison, R. M., and Achterberg, E. P.: Changes in iron speciation following a Saharan dust event in the tropical North Atlantic Ocean, *Mar Chem*, 110, 56–67, doi:10.1016/j.marchem.2008.02.006, 2008.
- Rinaldi, M., Decesari, S., Carbone, C., Finessi, E., Fuzzi, S., Ceburnis, D., O'Dowd, C. D., Sciare, J., Burrows, J. P., Vrekoussis, M., Ervens, B., Tsigaridis, K., and Facchini, M. C.: Evidence of a natural marine source of oxalic acid and a possible link to glyoxal, *J. Geophys. Res.-Atmos.*, 116, D16204, doi:10.1029/2011Jd015659, 2011.
- Schepanski, K., Tegen, I., and Macke, A.: Saharan dust transport and deposition towards the tropical northern Atlantic, *Atmos. Chem. Phys.*, 9, 1173–1189, doi:10.5194/acp-9-1173-2009, 2009.
- Schulz, M., Prospero, J. M., Baker, A. R., Dentener, F., Ickes, L., Liss, P. S., Mahowald, N. M., Nickovic, S., Garcia-Pando, C. P., Rodriguez, S., Sarin, M., Tegen, I., and Duce, R. A.: Atmospheric transport and deposition of mineral dust to the ocean: Implications for research needs, *Environ. Sci. Technol.*, 46, 10390–10404, doi:10.1021/Es300073u, 2012.
- Sciare, J., Oikonomou, K., Cachier, H., Mihalopoulos, N., Andreae, M. O., Maenhaut, W., and Sarda-Estève, R.: Aerosol mass closure and reconstruction of the light scattering coefficient over the Eastern Mediterranean Sea during the MINOS campaign, *Atmos. Chem. Phys.*, 5, 2253–2265, doi:10.5194/acp-5-2253-2005, 2005.
- Sciare, J., Favez, O., Sarda-Estève, R., Oikonomou, K., Cachier, H., and Kazan, V.: Long-term observations of carbonaceous aerosols in the Austral Ocean atmosphere: Evidence of a biogenic marine organic source, *J. Geophys. Res.-Atmos.*, 114, D15302, doi:10.1029/2009jd011998, 2009.
- Sullivan, R. C., Guazzotti, S. A., Sodeman, D. A., Tang, Y. H., Carmichael, G. R., and Prather, K. A.: Mineral dust is a sink for chlorine in the marine boundary layer, *Atmos. Environ.*, 41, 7166–7179, doi:10.1016/j.atmosenv.2007.05.047, 2007.
- Tesche, M., Gross, S., Ansmann, A., Müller, D., Althausen, D., Freudenthaler, V., and Esselborn, M.: Profiling of Saharan dust and biomass-burning smoke with multiwavelength polarization Raman lidar at Cape Verde, *Tellus B*, 63, 649–676, doi:10.1111/j.1600-0889.2011.00548.x, 2011.
- Tilgner, A. and Herrmann, H.: Radical-driven carbonyl-to-acid conversion and acid degradation in tropospheric aqueous systems studied by CAPRAM, *Atmos. Environ.*, 44, 5415–5422, doi:10.1016/j.atmosenv.2010.07.050, 2010.
- Turpin, B. J., Saxena, P., and Andrews, E.: Measuring and simulating particulate organics in the atmosphere: problems and prospects, *Atmos. Environ.*, 34, 2983–3013, 2000.
- van Pinxteren, D., Brüggemann, E., Gnauk, T., Müller, K., Thiel, C., and Herrmann, H.: A GIS based approach to back tra-

- jectory analysis for the source apportionment of aerosol constituents and its first application, *J. Atmos. Chem.*, 67, 1–28, doi:10.1007/s10874-011-9199-9, 2010.
- Virkkula, A., Teinilä, K., Hillamo, R., Kerminen, V.-M., Saarikoski, S., Aurela, M., Viidanoja, J., Paatero, J., Koponen, I. K., and Kulmala, M.: Chemical composition of boundary layer aerosol over the Atlantic Ocean and at an Antarctic site, *Atmos. Chem. Phys.*, 6, 3407–3421, doi:10.5194/acp-6-3407-2006, 2006.
- Warneck, P.: In-cloud chemistry opens pathway to the formation of oxalic acid in the marine atmosphere, *Atmos. Environ.*, 37, 2423–2427, doi:10.1016/S1352-2310(03)00136-5, 2003.
- Williams, J., de Reus, M., Krejci, R., Fischer, H., and Ström, J.: Application of the variability-size relationship to atmospheric aerosol studies: estimating aerosol lifetimes and ages, *Atmos. Chem. Phys.*, 2, 133–145, doi:10.5194/acp-2-133-2002, 2002.
- Yao, X. H., Fang, M., and Chan, C. K.: Size distributions and formation of dicarboxylic acids in atmospheric particles, *Atmos. Environ.*, 36, 2099–2107, 2002.
- Yao, X. H. and Zhang, L. M.: Chemical processes in sea-salt chloride depletion observed at a Canadian rural coastal site, *Atmos. Environ.*, 46, 189–194, doi:10.1016/j.atmosenv.2011.09.081, 2012.